

**BEARING RESPONSE TEST FOR THE POLYMER MATRIX COMPOSITE
LAMINATES: OPTIMIZATION OF DISPLACEMENT GAGE POSITION**

A Thesis by

Mohan Mittur Narayana

B.E., B.I.T Visvesvariah Technological University, 2005

Submitted to the Department of Mechanical Engineering
and the faculty of the Graduate School of
Wichita State University
in partial fulfillment of
the requirements of the Degree of
Master of Science

May 2008

© Copyright 2008 by Mohan Mittur Narayana,

All Rights Reserved

**BEARING RESPONSE TEST FOR THE POLYMER MATRIX COMPOSITE
LAMINATES: OPTIMIZATION OF DISPLACEMENT GAGE POSITION**

The following faculty have examined the final copy of this thesis for the form and content, and recommend that it be accepted in partial fulfillment of the requirement for the degree of Master of Science with a major in Mechanical Engineering.

Hamid Lankarani, Committee Chair

Ramazan Asmatulu, Committee Member

Krishna Krishnan, Committee Member

DEDICATION

To my dear **Nanjamma**
and
to all my dearest **friends**

ACKNOWLEDGMENTS

I would like to present my sincere appreciation to my graduate advisor, Dr. Hamid Lankarani, Professor of Mechanical Engineering, for his support, cooperation, and timely guidance throughout my graduate studies at Wichita State University. I would also like to thank Dr. Ramazan Asmatulu for inspecting my work and helping me to make this thesis better. My deepest gratitude to Dr. Krishna Krishnan for his cooperation and support. My sincere gratitude to Mr. Jason yeoh for providing me with testing equipment and supporting me to a wider extend for completing the experimental study in Structures Lab, National Institute for Aviation Research. My special thanks to Mr. Shin Mah for his continuous guidance, advice and support while working in the Structures Laboratory at NIAR. Finally, I would like to thank all my friends, colleagues for their cooperation all through my thesis work.

ABSTRACT

This thesis deals with composite joints with single shear tensile loading for a single piece specimen. The bearing response data from single shear test using a single piece specimen has been extensively used in the development of design allowable data. The first objective of the work was to test three different displacement gage position configurations for determining the bearing chord modulus and the 2% offset strength of composite coupons. Testing was done according to ASTM D5961: Procedure 'C'- the standard test procedure for the bearing response of a single shear one piece polymer matrix composite laminate. The Procedure 'C' testing method is not yet standardized by the ASTM and there is a great deal of confusion in the extensometer position. Hence, an attempt has been made to study the variability in the chord modulus, and more importantly the 2% offset bearing strength depending on the different reference positions of the displacement gage placement.

The other aim of thesis was to build a finite element (FE) model for a quasi isotropic material, to justify the FE results with experimental results, and then to conduct a set of parametric studies to study the stiffness behavior in all the three positions. The statistical analysis using Design of Experiments (DOE) of the parametric study data, identified significant factors affecting the results.

TABLE OF CONTENTS

Chapter	Page
1. INTRODUCTION.....	1
1.1 Composites Background.....	1
1.2 Bolted Joints.....	2
1.3 Composite Joint Failure Modes	3
1.4 Statement of work.....	4
1.5 Mission statement	5
1.6 Approach.....	5
2. LITERATURE REVIEW	7
2.1 Methods to Study Bearing Behavior.....	7
2.2 ASTM D5961 Test Method	12
3. EXPERIMENTAL PROCEDURE	13
3.1 Coupon Preparation	13
3.1.1 Fiber material selected	13
3.1.2 Test Coupon geometry	14
3.1.3 Number of Plies and Lay up Arrangement	14
3.1.4 Materials and test plan	15
3.2 Coupon Fabrication.....	16
3.3 Fixture and Coupon Mounting.....	16
3.4 Bearing Test Procedure.....	18
3.5 Data Reduction.....	19
4. EXPERIMENTAL RESULTS AND DISCUSSIONS	21
4.1 Material Comparison and Different Gauge Positions.....	22
4.1.1 Carbon fabric plain weave material	22
4.1.2 E-glass fabric material	27
4.2 Comparison of Carbon Plain Weave Fabric and E-glass Fabric.....	32
4.3 Rotation Factor.....	33
5. COMPUTATIONAL STUDY	35
5.1 Introduction.....	35
5.2 Approach.....	35
5.3 FE Model	35
5.4 Boundary Conditions and Material Properties.....	36
5.5 Material Model.....	37
5.6 Results and Discussion	37

TABLE OF CONTENTS (Continued)

Chapter	Page
5.7 Parametric Study	40
6. STATISTICAL ANALYSIS OF COMPUTATIONAL DATA.....	42
6.1 Statistical Design Matrix.....	43
6.2 Statistical Output Analysis.....	43
6.2.1 ANOVA output for bearing chord stiffness.....	44
6.2.2 Residual analysis for delamination depth	44
6.2.3 Factor effects of bearing chord stiffness.....	47
7. CONCLUSIONS AND RECOMMENDATIONS	50
7.1 Conclusions.....	50
7.2 Recommendations.....	51
8. REFERENCES	53

LIST OF TABLES

Table		Page
1	Laminate configuration for plain weave fabric materials	15
2	Test matrix	15
3	Statistical design matrix	43
4	ANOVA table for bearing chord stiffness	44

LIST OF FIGURES

Figure		page
1	Test configurations for bearing response [1]	2
2	Bolt shearing modes with respect to joint classification [5]	3
3	Modes of bearing failure [5]	3
4	Set up of Single shear for one piece specimen test [1]	4
5	Overview of the reference positions	6
6	Type of material: (a) Carbon plain weave fabric; (b) E – Glass fabric.....	13
7	Standard specimen for single shear [1]	14
8	Fabricated single shear specimen.....	16
9	Isometric view of the single shear (Procedure ‘C’) test fixture	16
10	Assembly of the fastener.....	17
11	Assembly of specimen and displacement gages on the fixture.....	17
12	Clip gage: Displacement gage used for the ASTM proposed method.....	18
13	Extensometer: Displacement gage used for in use procedure	18
14	Displacement gage mounted on the test setup	19
15	Tested single shear specimen.....	19
16	Stress vs. strain curve as illustrated in ASTM standard [1]	20
17	Load vs. deformation	21
18	Bearing stress vs. bearing strain.....	21
19	Load vs. deformation curve at reference position 1 for carbon fabric.....	22
20	Bearing stress vs. bearing strain curve at reference position 1 for carbon fabric	23
21	Load vs. deformation curve at reference position 2 for carbon fabric.....	23
22	Bearing stress vs. bearing strain curve at reference position 2 for carbon fabric	24
23	Load vs. deformation curve at reference position 3 for carbon fabric.....	24
24	Bearing stress vs. bearing strain curve at reference position 3 for carbon fabric	25
25	Bearing stress vs. bearing strain curves for all the three reference positions for carbon fabric	25
26	Bearing chord stiffness compared between three reference positions for carbon fabric	26
27	2 % offset bearing strength compared between three reference positions for carbon fabric.....	26
28	Load vs. deformation curve at reference position 1 for glass fabric.....	27
29	Bearing stress vs. bearing strain curve at reference position 1 for glass fabric	27
30	Load vs. deformation curve at reference position 2 for glass fabric.....	28
31	Bearing stress vs. bearing strain curve at reference position 2 for glass fabric	28
32	Load vs. deformation curve at reference position 3 for glass fabric.....	29
33	Bearing stress vs. bearing strain curve at reference position 3 for glass fabric	29
34	Bearing stress vs. bearing strain curves for all the three reference positions for glass fabric	30
35	Bearing chord stiffness compared between three reference positions for glass fabric	31
36	2 % offset bearing strength compared between three reference positions for glass fabric.....	31

LIST OF FIGURES (Continued)

Figure	Page
37	Bearing chord stiffness comparison between two materials and three reference positions32
38	2 % offset bearing strength comparison between two materials and three reference positions33
39	Load vs. actuator deformation & hole deformation for old procedure34
40	Load vs. actuator deformation & hole deformation for proposed procedure34
41	Two dimensional Finite element model.....36
42	FE model with boundary conditions36
43	Distribution of Von mises stress around the hole region37
44	Y-strain distribution in the FE analyzed model38
45	bearing strain vs. stress difference between the three reference positions39
46	bearing chord stiffness compared between the experimental and FE data for all the three positions.....39
47	bearing chord stiffness vs. reference positions for end distance ratio40
48	bearing chord stiffness vs. reference positions for pitch distance ratio41
49	Normal probability plot: Bearing chord stiffness45
50	Outliner plot: Bearing chord stiffness45
51	Residuals vs. Parameter ratio: Bearing chord stiffness.....46
52	Residual vs. reference positions: Bearing chord stiffness46
53	Effect of reference positions on bearing chord stiffness for $e/d = 2$47
54	Effect of reference positions on bearing chord stiffness for $e/d = 3$47
55	Effect of reference positions on bearing chord stiffness for $e/d = 4$48
56	Effect of reference positions on bearing chord stiffness for $w/d = 4$48
57	Effect of reference positions on bearing chord stiffness for $w/d = 6$49
58	Effect of reference positions on bearing chord stiffness for $w/d = 8$49

LIST OF ABBREVIATIONS

ASTM	American Society of Testing and Materials
CFRP	Carbon Fiber Reinforced Polymer
GFRP	Glass Fiber Reinforced Polymer
NIAR	National Institute for Aviation Research
SL	Slope line
OSL	2% offset slope line
2D	Two dimensional
FE	Finite element
COR	Coefficient of restitution
ADINA	Automatic Dynamic Incremental Nonlinear Analysis
ANOVA	Analysis of variance
MTS	Materials testing solutions
DOE	Design of experiments

LIST OF SYMBOLS

d	Fastener or pin Diameter
D	Hole diameter
F^{bru}	Yield Bearing Strength
H	Thickness range
E	Edge distance
K	Hole Factor
L	Length
P^{Max}	Maximum Load
W	width
X	Global x-direction
Y	Global y-direction
Z	Global z-direction

CHAPTER 1

INTRODUCTION

1.1 Composites Background

Composites are being extensively used in aircraft industries. Their weight saving property is the main driving force along with other benefits like good fatigue and corrosion resistance properties. A clear trend is that composites are used increasingly in heavily loaded primary structures. The increasing use of Composite materials and its popularity has prompted significant research effort aiming at developing reliable design methods.

Designing useful structures means that several parts must be joined together. This can be done by adhesive joining, mechanical joining or hybrid joining which is a combination of the first two techniques. With low weight and good sealing properties the adhesive joints have advantage over the mechanical joints but transferring high loads is not very effective due to high interlaminar stresses in composites. Also the adhesive joints are sensitive to environmental conditions and adhesive structures cannot be easily disassembled while replacing the damaged parts.

Mechanical joining, i.e. using fasteners, is the most important method in the aerospace industry. Although it's most preferred in most of the cases it's associated with difficulties. The presence of a hole in the laminate disturbs the stress field. Stresses are concentrated at the vicinity of the hole. Introduction of the fastener into the hole and the resultant load through the contact between the fastener and the hole surface will make the stress concentration even more severe. This makes the bolted joint as a weak link in the composite structure, which must be properly designed to achieve an efficient structure. Significant research has been done for last

few decades, aiming at developing reliable design methods. These design methods are imperative in order to achieve safe structures with optimum performance.

Application of composite materials in an aircraft requires detailed knowledge about their behavior, like strength of joints and the mode in which they fail. Fundamental investigations on joint strength have been conducted using simple test objects. Three basic types of test configurations are illustrated in figure 1.

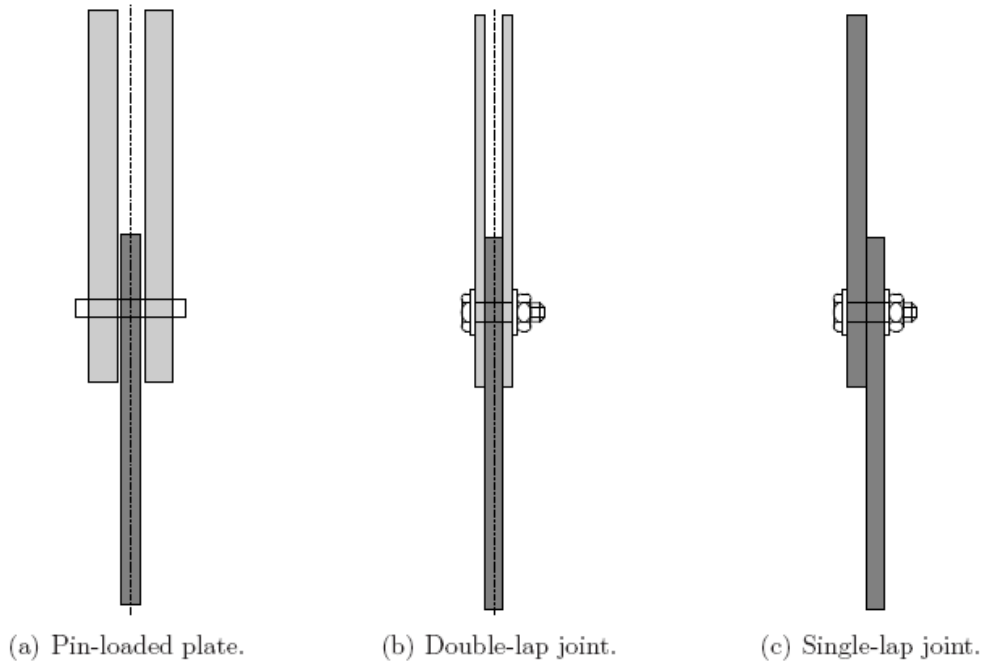


Figure 1 Test configurations for bearing response [1]

1.2 Bolted Joints

Single shear and double shear joints are two types of bolted joints as shown in figure 2. In these two types of joints the opposition to the load acting is by single and double cross sections respectively. This makes the bearing strength in double shear joints to be twice compared to single shear joints. The bearing deformation at the laminate hole is at the point of contact between hole and fastener.

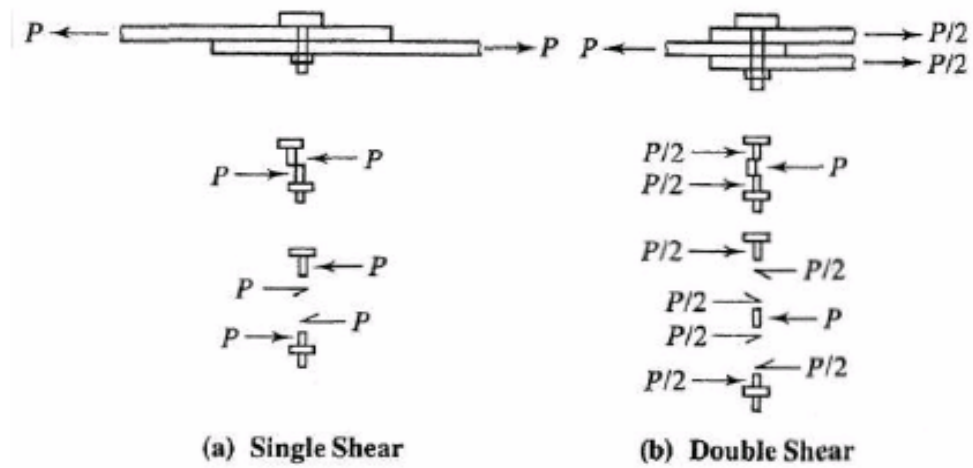


Figure 2 Bolt shearing modes with respect to joint classification [5]

1.3 Composite Joint Failure Modes

The failure modes in bolted composite are as shown in figure 3.

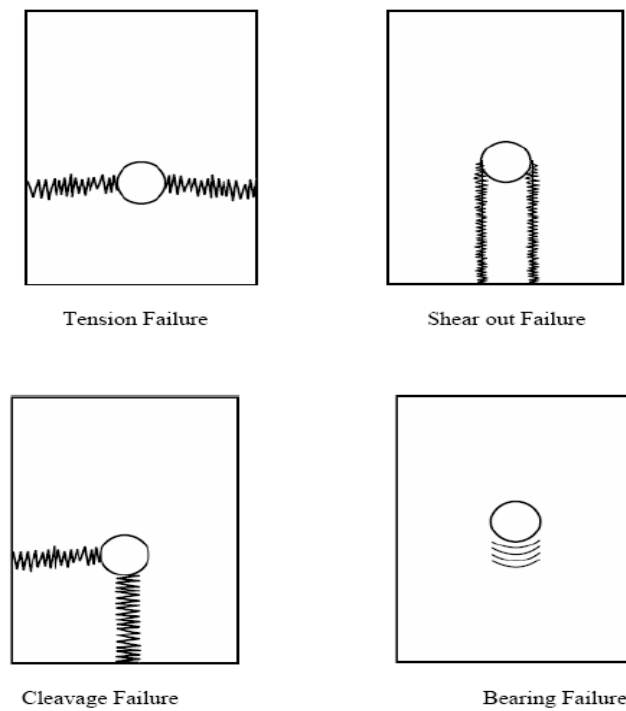


Figure 3 Modes of bearing failure [5]

1.4 Statement of Work

This thesis deals with testing carbon fiber (CFRP) and glass fiber (GFRP) composite laminate specimens at their coupon level to find their bearing stiffness and 2% offset strength and hence optimizing the displacement gauge placement in single shear joints in conformation to the ASTM D5691 procedure 'C'. This study also aimed at comparing the method which is in practice to the newly proposed method by ASTM for procedure 'C'. The test matrix consisted of quasi isotropic plain weave carbon fabric and E-Glass fabric. They were again classified into three positions according to the displacement gauge placements.

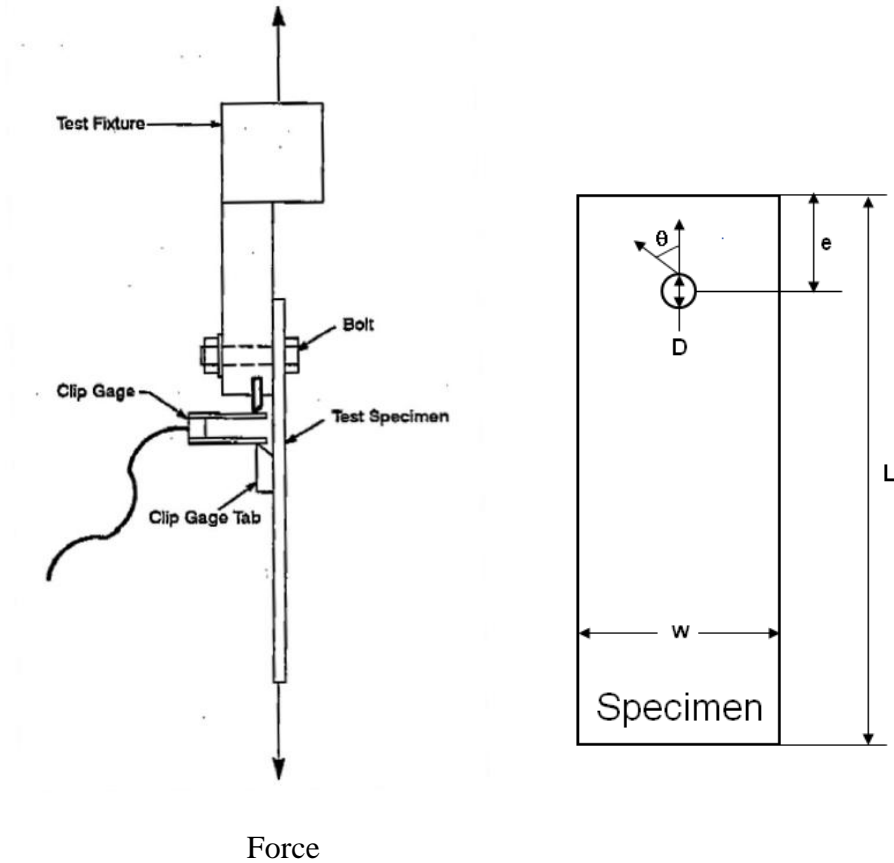


Figure 4 Set up of Single shear test for one piece specimen [1]

W – Specimen Width, e – Specimen edge to hole distance and D – Hole Diameter.

A simple schematic shows the setup for a single shear in above figure 4. The composite coupon with certain clamp up force is fastened on to the hardened steel fixture.

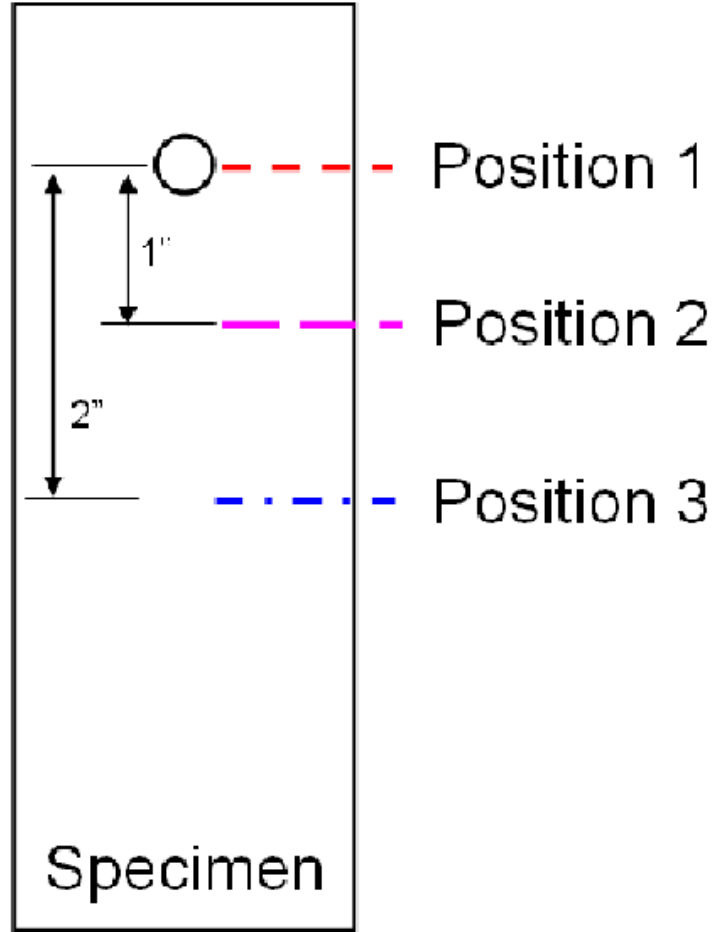
1.5 Mission Statement

The objective of this thesis is to optimize the displacement gage placement in single shear test for bearing response by investigating the following:

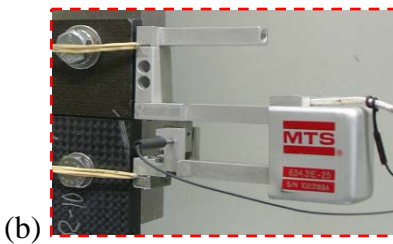
- Investigate the bearing deformation by measuring at different reference positions on the testing specimen i.e., compare the old method and the proposed method
- Compare the bearing stiffness modulus between the different reference positions
- Compare the 2% offset bearing strength between different reference positions
- Study the rotation factor affecting the results comparing the two methods
- Development and validation of the FE model
- Parametric study on FE model
- Statistically analyzing the FE data from parametric study

1.6 Approach

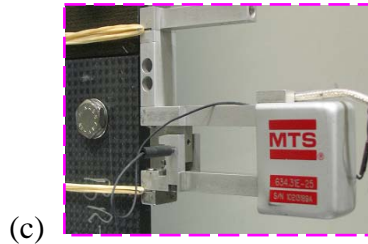
When testing bolted joints the interpretation of test results for bolted joints mainly depends on the method used to generate the load-displacement response curves. While the load is measured using a load cell, which can be trusted but its not same in the case for displacement, which is mainly measured using displacement gages like extensometers, clip gages etc.,[2] Its not the problem with the displacement gages rather with the choice of the reference points for the displacement measurement. The deformations that are measured actually depend of the reference points of the displacement gages. In this study the reference points are considered as the reference positions. The figure 5: (a) shows all the three reference positions.



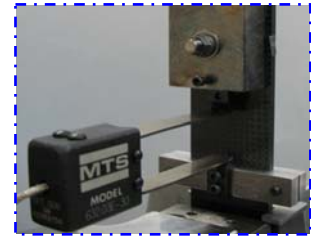
(a)



(b)



(c)



(d)

Figure 5 Overview of the reference positions;(a) Positions shown on the specimen;(b) View of displacement gage placement in position1;(c) View of displacement gage placement in position2;

(d) View of displacement gage placement in position3 (Courtesy: NIAR, Structures Lab)

CHAPTER 2

LITERATURE REVIEW

This chapter provides a review of the work done to study the bearing deformation and displacement gauge placement for polymeric matrix composite materials and the various parameters affecting the bearing deformation characteristics. The research gives a brief insight into experimental as well as the analytical methods such as finite element methods addressing this problem.

2.1 Methods to Study Bearing Behavior

Various experiments were done to the minute details to determine bearing response on composite joints and their effects on bearing properties considering different parameters. The single shear, double shear and bypass tests were the most important among them. This thesis aimed at studying the single shear test joint particularly ASTM D5961 procedure 'C' which is also called as single shear for one piece specimen.

B. Vangrimde and R. Boukhili [2] setup a procedure to measure the bearing stiffness of a GFRP laminate in a single-bolt double lap joint. With a finite element model they showed that the bolt and the fixture deformations affect the stiffness results. The experimental displacement data was corrected before calculating the coupon deformation. The coupon bearing stiffness was also simulated by a two-dimensional finite element model in ANSYS. The bolt was modeled as a rigid cylindrical target surface. The contact between the hole and the bolt was modeled with 2D flexible contact surface to rigid target surface.

The rigid body bolt was fixed and a 0.4 mm displacement was applied 100 mm from the hole center. The bolt-hole clearance of 0.3mm and friction μ of 0.33 were taken into account for the analysis.

The coupon deformation was studied in detail to remove the ambiguity and so a meaningful displacement measure can be devised. In this study the author studied bearing coupon deformation not the hole deformation which is considered in ASTM D5961 test method. Parameters like pitch distance ratio w/d and end distance ratio e/d was also studied. The results showed that the coupon displacement decreases when the plate width increases, although the decrease in displacement gets less as width increases. The authors measured the displacement from a displacement where there was uniform stress field. There was good agreement observed between experimental results considering hole clearance, material non linearity and bolt-hole friction.

Finally authors came into a conclusion that coupon bearing deformation is of practical interest not the hole elongation to the engineer since it allows a convenient calculation of the total displacement.

A combined research on double lap carbon fiber/epoxy quasi-isotropic composite was done by Camanho and Matthews [3]. They used the progressive damage approach to build the finite element model. They used a quarter symmetric model and their each ply was modeled using eight node solid elements and the model was based on displacement formulation. The aim was to study on the modes of failure, the strengths and stress analysis.

Failure modes and strength values were perfectly predicted by their experiments. They were able to predict the ultimate bearing strength of the material, by defining the failure from other design factors.

Takaka [4] modeled to study the pure bearing strength and clamping pressure on the composite materials. There assumption was that the material failing under the bearing mode at the contact surface is not compressed by the constraint offered by washer clamped at the hole.

The three dimensional model was developed using ABAQUS. The model is built on a progressive failure approach. The author [4] determined that the stiffness of the materials tends to decrease as the compressive loads are applied on the bearing surface. However the clamp up force applied helps to support the surrounding surface, which helps in counter reacting the compressive loads.

A.J Nicola and Fantle did Evaluation of bearing clearances using carbon fiber composites. A double lap shear test was conducted on a quasi-isotropic laminate with eight plies and laminates with $\pm 45^\circ$ orientations, with out any clamping torque. This test was aimed at studying the varying clearances between 0.000 in and 0.006 in.

The experiments showed that the results were higher for quasi-isotropic specimens when compared to the 45° orientation laminates and the 4% hole deformation strength was less by 30%.

Counts and Johnson [5] studied the effects of temperature on the ultimate bearing strength. The specimens considered for the experiment were quasi-isotropic laminates made up of 64 plies. The experiment was conducted for hot, cold and room temperatures, the three temperature levels being 350° F, -58° F and 75° F. To induce more bearing stresses and to keep same bolt loads two materials IM7/PETI-5 and IM7/K3B were tested using compression test. Research showed no matter how the specimens were loaded in tension or compression it has no difference in there bearing strength. It showed that the ultimate bearing strength increased with decrease in temperature and vice versa. However the bearing failure was much faster at lower temperatures. The NDE inspection on these specimens revealed that 0° plies cracked and there was buckling at 45° and 90° plies.

Smith along with Pasoe [7] did pin bearing analysis for strength on carbon fiber reinforced polymer laminates. Cap head fasteners were used for the experiment. A clamp up torque of 0-23 N-m was used and damage on the loading surface was studied using electron microscope. The results showed that composite panels with 0° plies on the outer surface showed a tendency of splitting and breaking of layers. On the contrary, panels with 0° ply in the inner surface showed delamination between the layers. Some interlamination shearing was observed when the layers had an angular difference of 90° when compared with the ones which had an angular difference of 45° . The effect of different stacking sequence did not influence much on the glass fiber reinforced polymers laminates unlike the carbon fiber reinforced polymers.

By using the washers to clamp with the torque of 20in-lbs its shown that the damage is slowed and the failure takes place at higher load [7]. This shows that higher torque constraints the delamination.

A study to compare the three failure modes was carried out by Crews and Naik [8]. They experimented a quasi isotropic T300/5208 graphite epoxy material of 16ply thickness. They also constructed a finite element model. Using the FE model they investigated the effects of various variables. They also found out the failure modes and the strengths respective to them using the FE model. Finite element model assumed a nonlinear problem due to the fastener hole clearances.

Takaki [9] studied various clamping configurations by constructing a 3D finite element model to predict the effects of clamp up forces. Their motive was to find out what influenced the clamp surface area on the hole, and stiffness of the fastener on the bearing strength. The results obtained from this study proved that their assumption made in their earlier study was true. They found out as the clamping area increases the more is bearing strength increases.

Shyprykevich [10] suggested various test methods for different types of bearing tests for single, double and bearing bypass along with fastener pull through. It was needed that the lay up order, laminate thickness and the fastener diameter selected did not break in the shear or net tension, with a clearance value of 0.000-0.0025. The fastener used was required to be only in finger tight condition. The method of failure and hole damage values are important in characterizing the bearing joint.

Jurf and Vinson [11] constructed a non linear finite element model to study the connection between width, edge distance hole thickness and washer size. The computer program ADINA was used to build the FE model. Their finite element results were similar to the experimental results.

2.2 ASTM 5961 Test Method

The ASTM D5961 [1] is a test method from ASTM particularly designed to determine the bearing response of composite laminates. The standard covers different procedures including the following:

- i. Procedure 'A' double shear test,
- ii. Procedure 'B' single shear test,
- iii. Procedure 'C' single shear test for single piece specimen.

With few alterations, the test method conforms to the MIL-HDBK-17 [10]. The simplified figure 4 represents the fixture type for single shear single-piece specimen experiment. The specimens were torqued at 35 in-lbs. They were tested at test speeds of 0.05 in/min. The one head constrains the test specimen in the grips whereas the other head is constant. The load is applied on the

specimen until the highest load is attained and the test is ended when the load reduces to 30% of the highest load.

CHAPTER 3

EXPERIMENTAL PROCEDURE

3.1 Coupon Preparation

This consists of following main stages.

- Type of fiber material selected
- Specimen geometry
- Number of plies used and lay up sequence decision
- Test matrix

3.1.1 Fiber material selected

Two different fiber materials were used for the testing

- CYTEC PWC T300 3KNT Plain Weave Carbon Fabric
- NEWPORT NB321/7781 FIBERGLASS

The main idea for selecting the above materials was to obtain good bearing response and also would give a wide range of difference in two materials.

- Carbon and glass fabric

Both the materials consist of fabric in which the fibers run perpendicular to each other which means the fibers run in both the major axes the longitudinal and the transverse direction. The fibers are lined up over and under one fiber at once. Fig. 6 shows the schematic for the fiber alignment in the Fabric material for both carbon and glass.

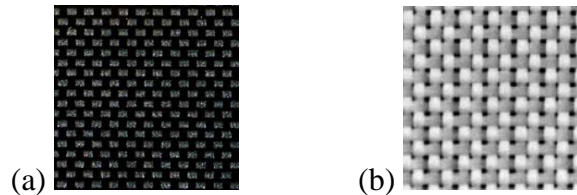


Figure 6 Type of material:

(a) Carbon plain weave fabric; (b) E – Glass fabric

3.1.2 Test coupon geometry

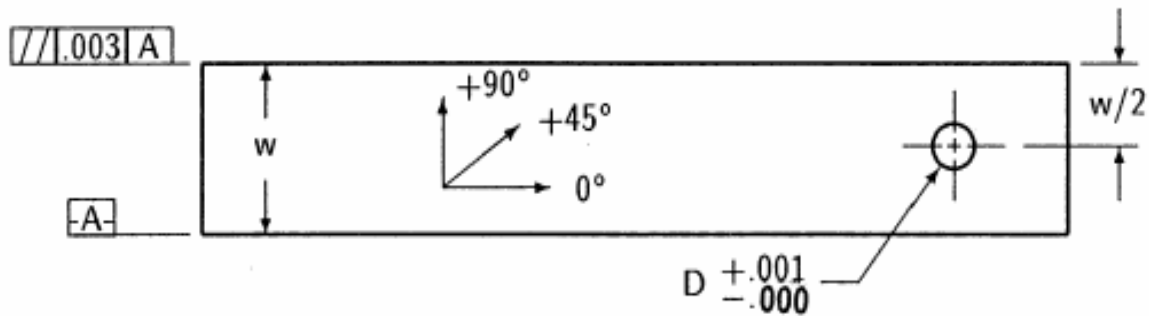


Figure 7 Standard coupon for procedure 'C' [1]

- Bolt Diameter (d) : 0.25 inch
- Coupon Hole diameter (D) : 0.250 inch
- Coupon Thickness range (h) : 0.08 to 0.208 inch
- Coupon Length (L) : 5.5 inch
- Width of the Coupon (w) : 1.5 inch
- Distance from Hole Center to Edge (e) : 0.75 inch

The Dimensions for the coupon geometry are in conformance with ASTM D5961 test method for the single shear one-piece specimen Procedure 'C' as shown in the figure 7.

3.1.3 Number of plies and lay up arrangement

The Arrangement and count of plies were finalized on the principle of percentage of different standard degrees in direction of plies as illustrated in figure 7. The lay up arrangement for both the materials are Quasi isotropic. This lay up was chosen in conformance to ASTM D5961 test standard for the procedure 'C'. Table 1 shows details of lay up arrangement and number of plies.

TABLE 1

LAMINATE CONFIGURATION FOR PLAIN WEAVE FABRIC MATERIALS

Material	Lay up % (0 ⁰ /45 ⁰ /90 ⁰)	Ply Stacking Sequence	Total Plies	Nominal Thickness (in)
Carbon fabric	25/50/25(Quasi)	[0/45/90/-45]2S	16	0.142
Fiber glass fabric	25/50/25(Quasi)	[0/45/90/-45] S	8	0.088

3.1.4 Materials and the test plan

The test plan consists of two different materials with identical lay up arrangement. Further each material was classified according to three different positions of displacement gage placement. The Table 2 shows two types of composite materials used with three different positions.

TABLE 2

TEST MATRIX

MATERIAL	LAYUP	DISPLACEMENT GAGE POSITION	NO. OF SPECIMENS
CYTEC PWC T300 3KNT Plain Weave Carbon Fabric	[0/45/90/-45] 2S	Position 1	3
		Position 2	3
		Position 3	3
NEWPORT NB321/7781 FIBERGLASS	[0/45/90/-45] S	Position 1	3
		Position 2	3
		Position 3	3
Total			18

3.2 Coupon Fabrication

The laminates were 15”x15” in dimension. All the specimens were cut along the 0⁰ direction of the plies using the milling cutter, edge grinded using grinding machine and drilled in the drilling machine. The fabricated specimen is as shown in the figure 8.



Figure 8 Fabricated Specimen

3.3 Fixture and Coupon Mounting

The test fixture is as shown below in the figure 9. The fixture has three holes a bigger diameter upper hole and smaller diameter fastener holes. The hole 1 as shown in the figure 9 connects to the universal joint which is fixed to the stationary head of the testing machine. The hole 2 is used to attach a tab which is used for fixing displacement gage. The hole 3 is used for fastening the specimen to the fixture i.e. the bearing hole. The fastener assembly is as shown in the figure 10.

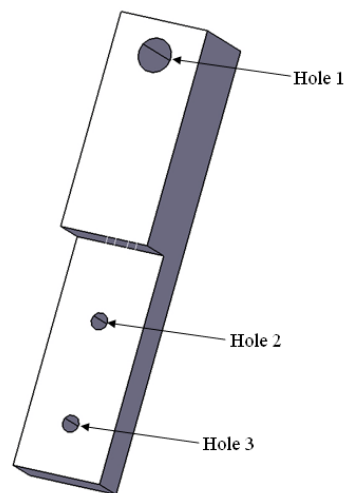


Figure 9 Isometric view of the single shear (Procedure ‘C’) test fixture



Figure 10 Assembly of the fastener
(Courtesy: NIAR)

The specimen is assembled on the fixture, then the displacement gages are fixed to the specimen and the specimen is gripped to the actuator in the MTS machine as shown in fig 11.

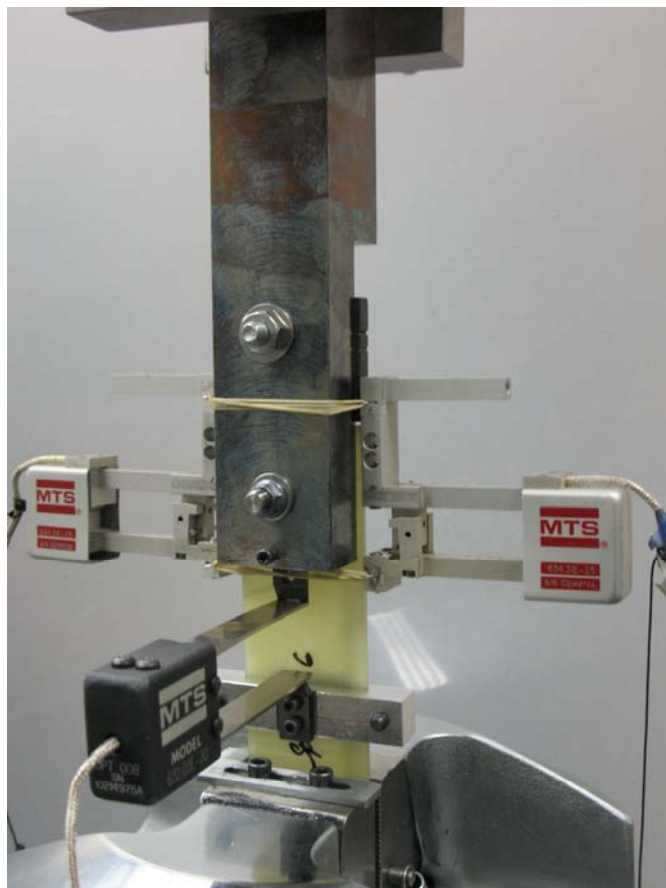


Figure 11 Assembly of specimen and displacement gages on the fixture
(Courtesy: NIAR)

3.4 Bearing Test Procedure

A Hydraulic load frame from MTS with a 22,000lb capacity is used for testing in conformance with the bearing standard test method ASTM D5961. The test rate is a uniform 0.05 in/min in conformance with ASTM standard. The grip pressure used to constraint the specimen is 2500 psi. The specimen is constrained on one side in the fixture hole with the bolt. The other end of the specimen is constrained in the wedges using specific amount of pressure.



Figure 12 Clip Gage: Displacement gage used for the proposed method
(Courtesy: NIAR)



Figure 13 Extensometer: Displacement gage used for old procedure
(Courtesy: NIAR)

To measure the hole distortion displacement gages were used with precise calibration. The displacement gages measure from -0.21 to a maximum range of +0.21 in inches. Figure 12 and 13 shows the clip gage and the extensometer respectively. The clip gage and the extensometers are mounted on the fixture as shown in the figure 14; (a) & (b) respectively. The extensometers are mounted with the help of rubber bands and the clip gage is mounted with the help of attachment.

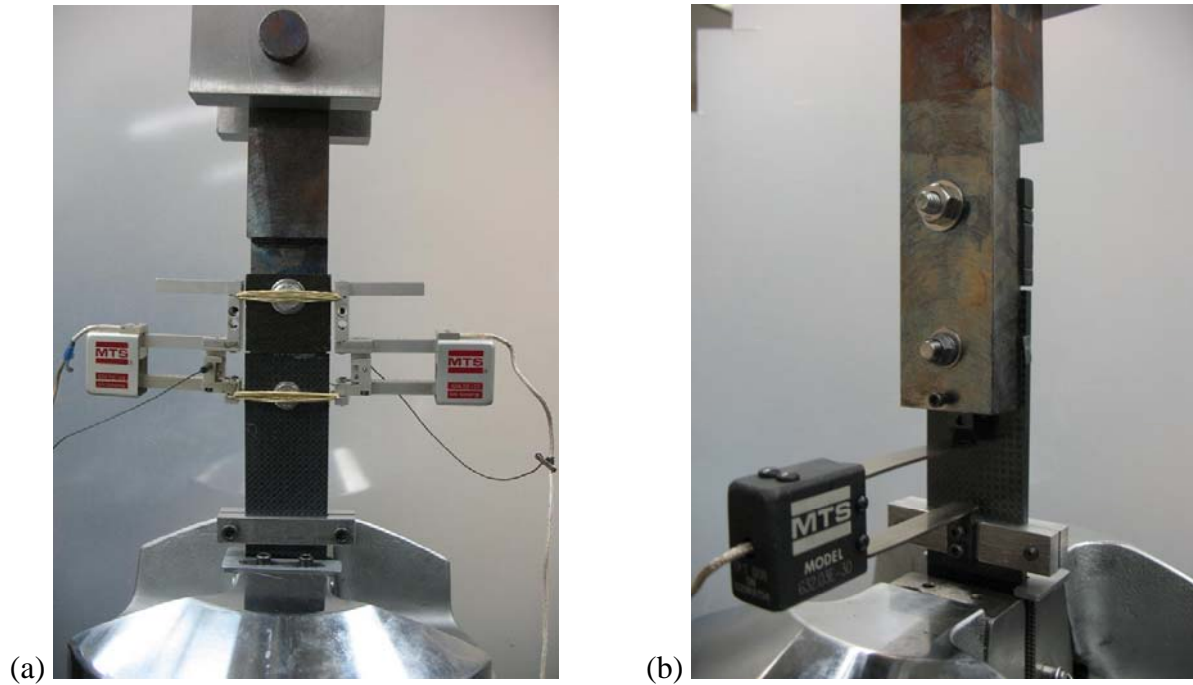


Figure 14 Displacement gage mounted on the test setup: (a) In use method; (b) Proposed method

3.5 Data Reduction

The results obtained from the MTS Testworks software which is used for data collection is in .txt format. The data with load, actuator and the displacement gage readings are obtained from Testworks. The tested specimen with the hole distortion is shown in figure 15.



Figure 15 Tested single shear specimen

The ultimate bearing strength and 2% offset bearing strength are the values to be attained from the testing. The peak bearing F^{bru} strength is determined using the equation

$$F^{bru} = P^{Max} / (K * D * H) \dots \dots \dots 1$$

In bearing single shear test the value of load factor ‘K’ is a constant 1. The 2% offset strength is obtained by offsetting the line 2% drawn along a linear part of the curve. The point where it bisects the stress vs. strain curve is the 2% offset strength.

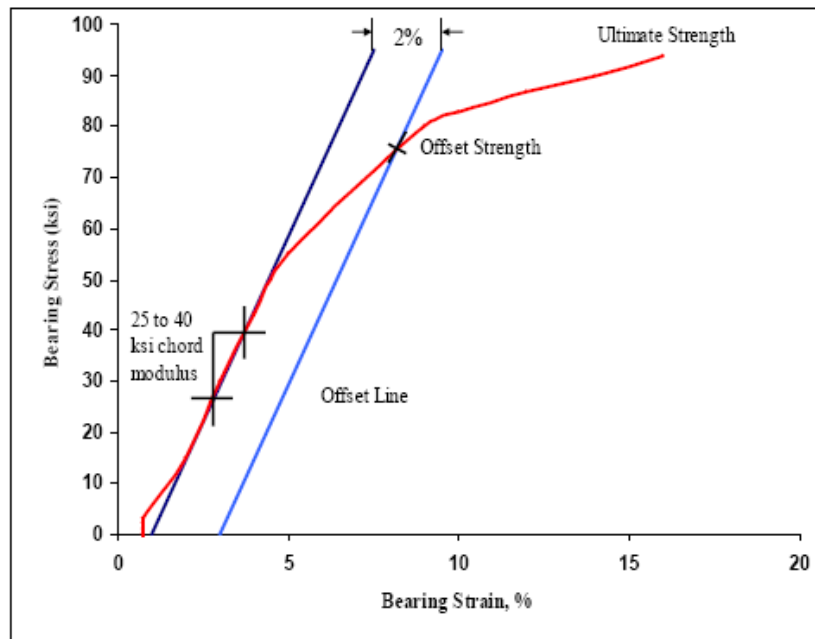


Figure 16 Stress vs. strain curve as illustrated in ASTM standard [1]

Figure 16 shows the standard stress vs. strain curve. The chord modulus is determined by calculating the slope from the curve. The data obtained from the text file is reduced with the built in macros for the bearing test. Figures 17 and 18 show the results determined from the test data solved in Microsoft Excel.

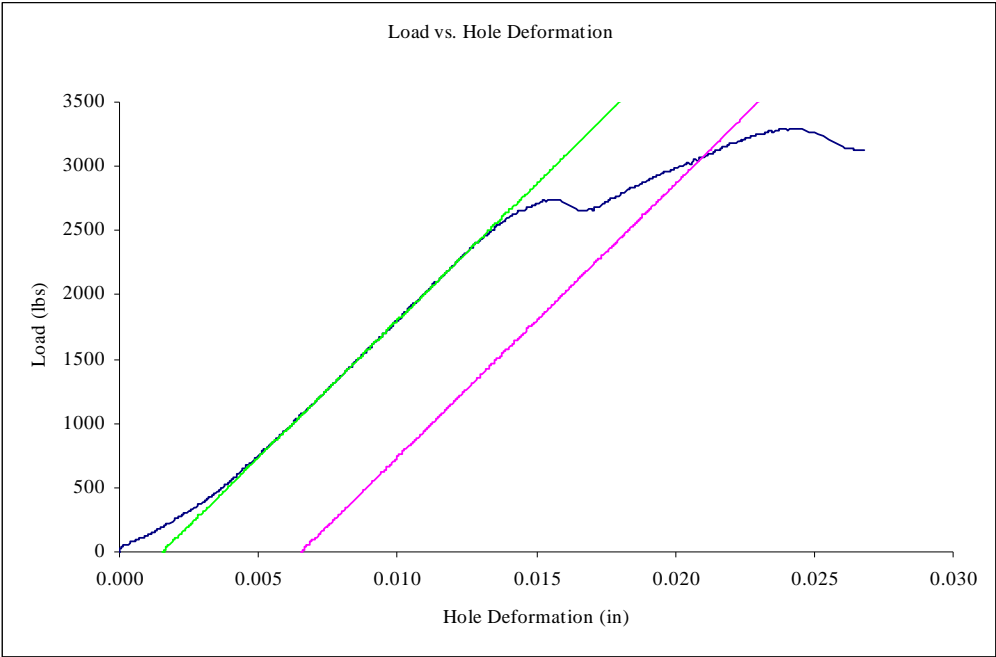


Figure 17 Load vs. deformation

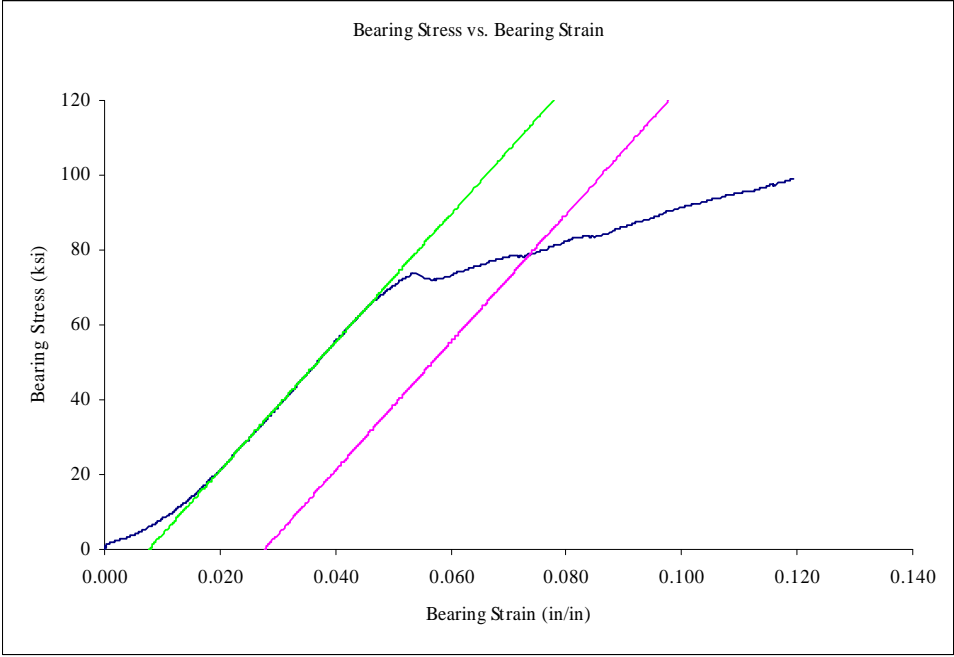


Figure 18 Bearing stress vs. bearing strain

CHAPTER 4

EXPERIMENTAL RESULTS AND DISCUSSIONS

The experimental study gives a good idea of how the bearing chord modulus and bearing strength changes by varying different positions of displacement gage placement on the testing specimen. The 2% strength value of the bearing joint is considered to be failure strength in aerospace. The bearing chord stiffness and its dependent 2% offset hole deformation strength were the main motto of these experiments.

The results for various parameters such as material types, different positions of displacement gages and failure modes have been discussed in this chapter.

4.1 Material Comparison and Different Gauge Positions

4.1.1 Carbon fabric plain weave material

Following are the load vs. deformation & stress vs. strain curves results for the reference position 1 as shown in figures 19 and 20.

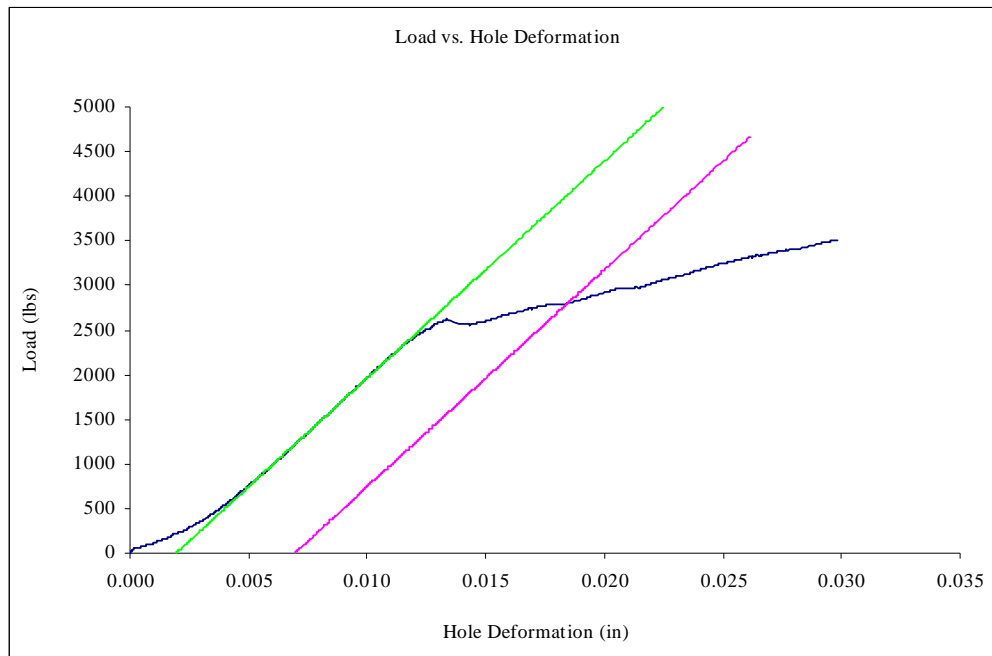


Figure 19 Load vs. deformation curve at reference position 1 for carbon fabric

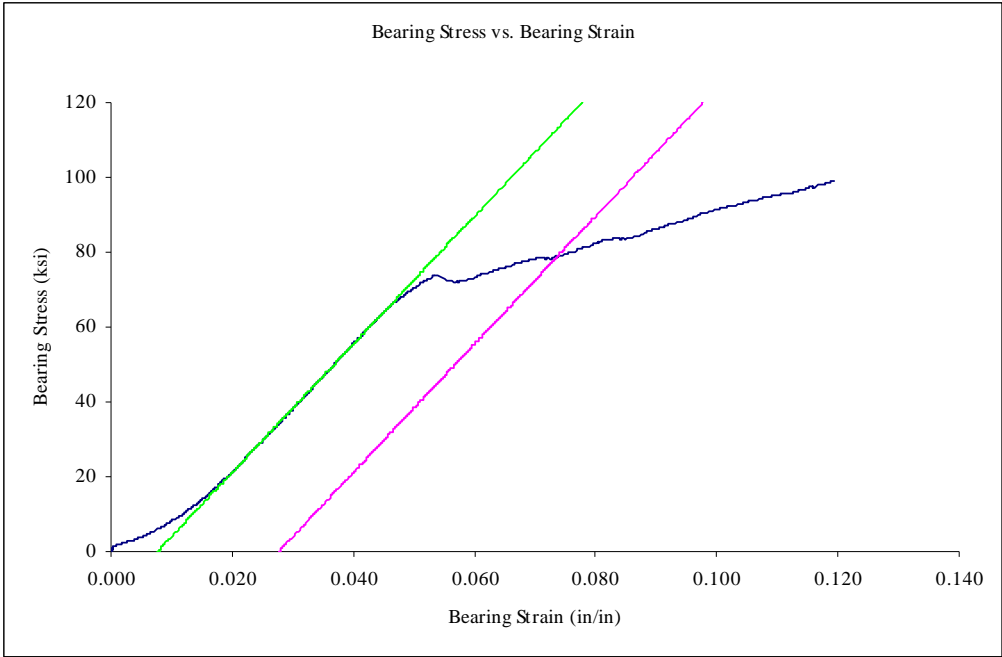


Figure 20 Bearing stress vs. bearing strain curve at reference position 1 for carbon fabric

Following are the load vs. deformation & bearing stress vs. bearing strain curves results for the reference position 2 as shown in figures 21 and 22.

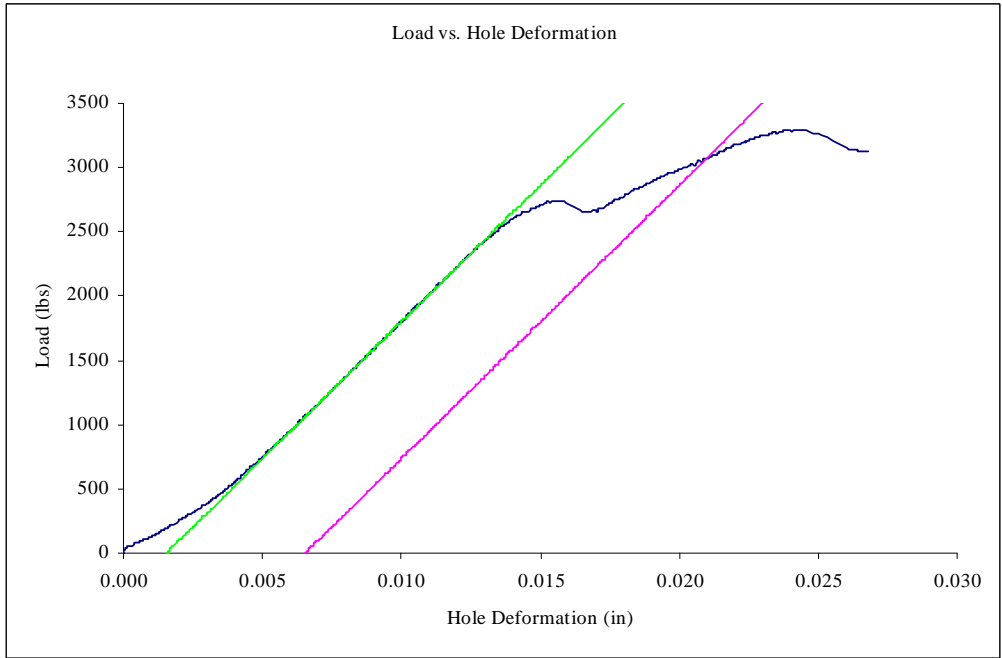


Figure 21 Load vs. deformation curve at reference position 2 for carbon fabric

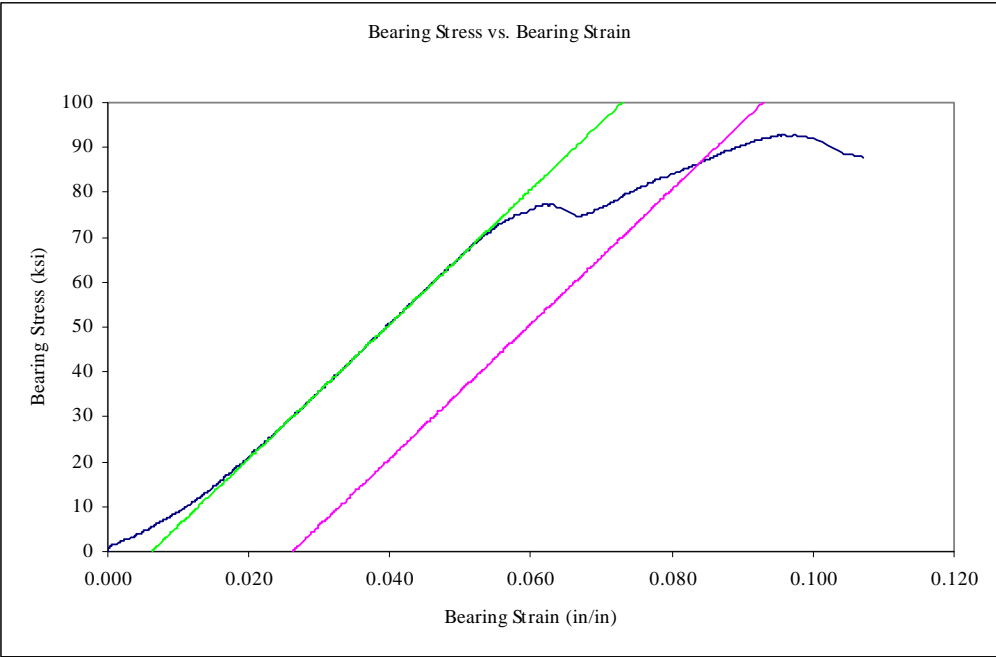


Figure 22 Bearing stress vs. bearing strain curve at reference position 2 for carbon fabric

Following are the load vs. deformation & bearing stress vs. bearing strain results for the reference position 3 as seen in figures 23 and 24.

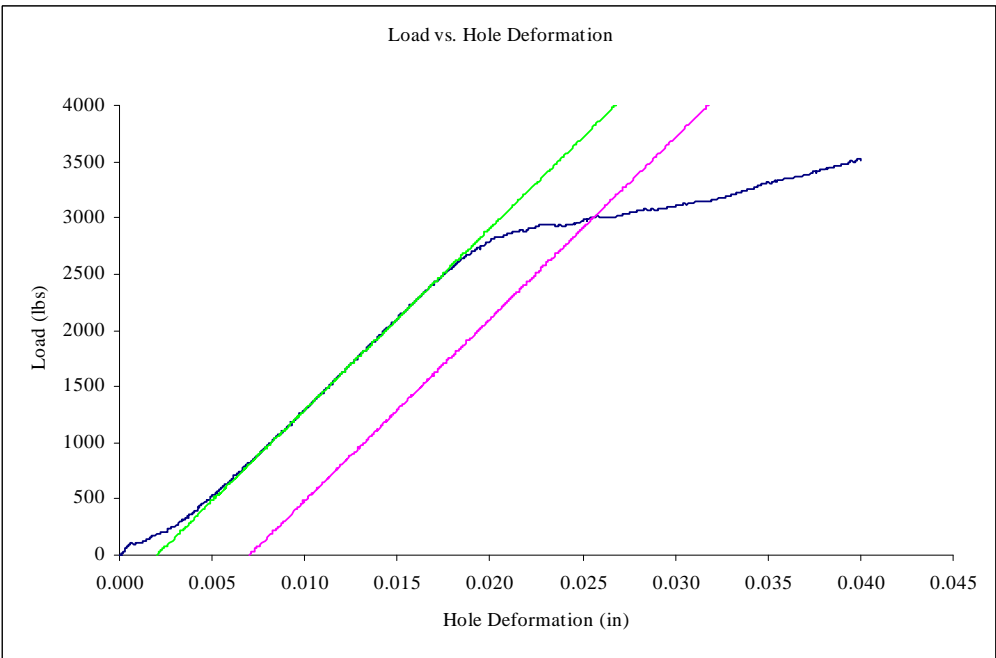


Figure 23 Load vs. deformation curve at reference position 3 for carbon fabric

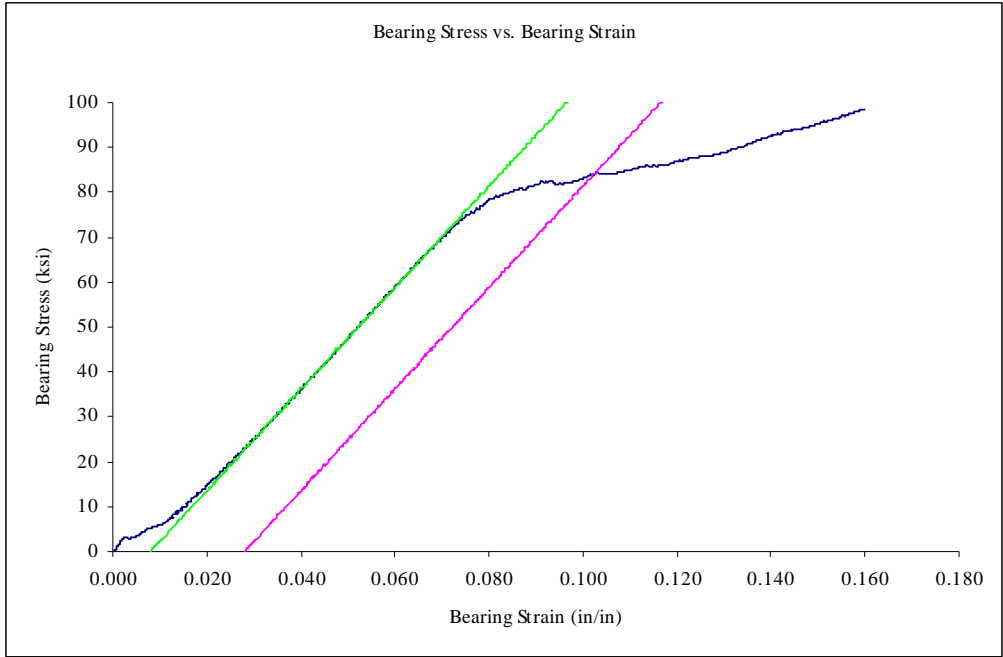


Figure 24 Bearing stress vs. bearing strain curve at reference position 3 for carbon fabric

Following are the bearing stress vs. bearing strain curve results for all the reference position 1, 2 and 3 as shown in figures 25.

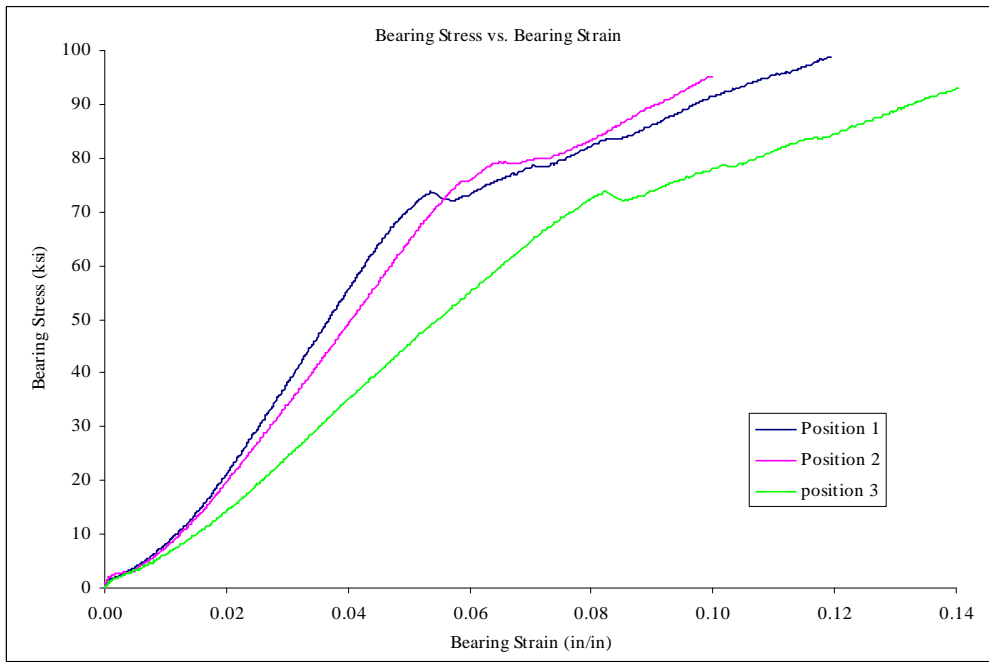


Figure 25 Bearing stress vs. bearing strain curves for all the three reference positions

The plain weave carbon fiber material is compared here for the bearing stiffness and the 2% offset bearing strength. The reference position 1 shows the maximum bearing stiffness and the reference position 3 shows the least bearing stiffness as shown in the figure 26. The 2% offset bearing strength remains same for all the three reference positions as shown in figure 27.

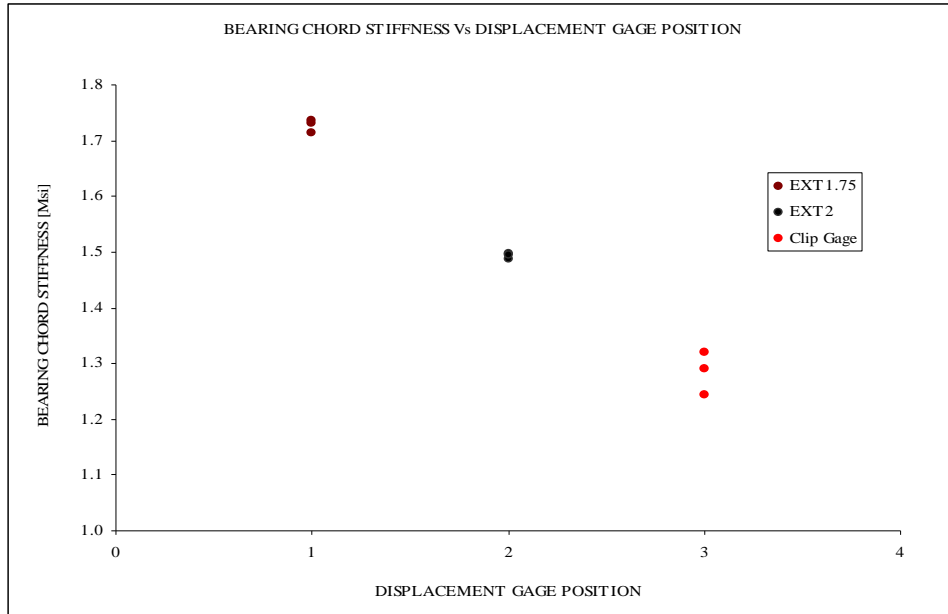


Figure 26 Bearing chord stiffness compared between three reference positions

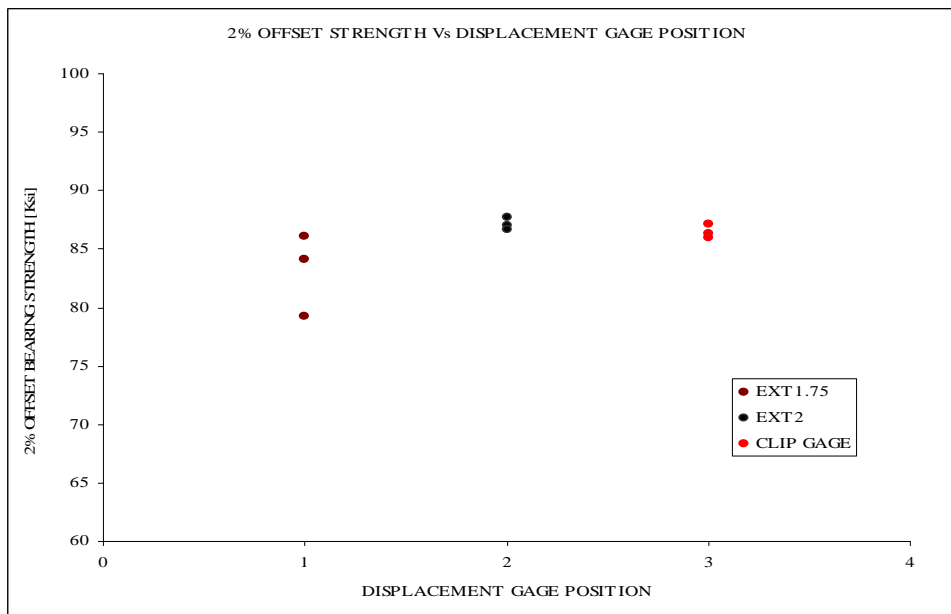


Figure 27 2% offset bearing strength compared between three reference positions

4.1.2 E-Glass fabric material

Following are the load vs. deformation & bearing stress vs. bearing strain curve results for the reference position 1 as shown in figures 28 and 29.

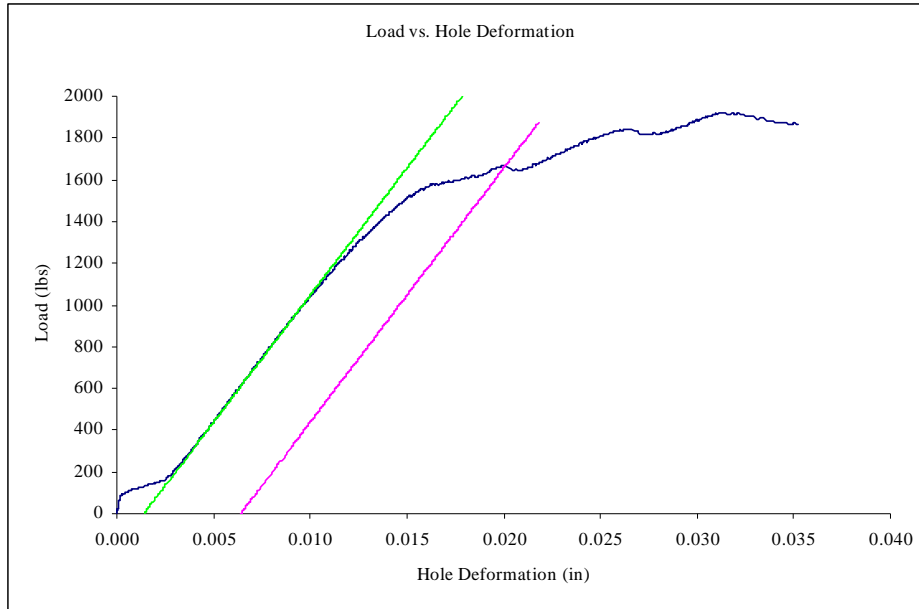


Figure 28 Load vs. deformation for reference position 1

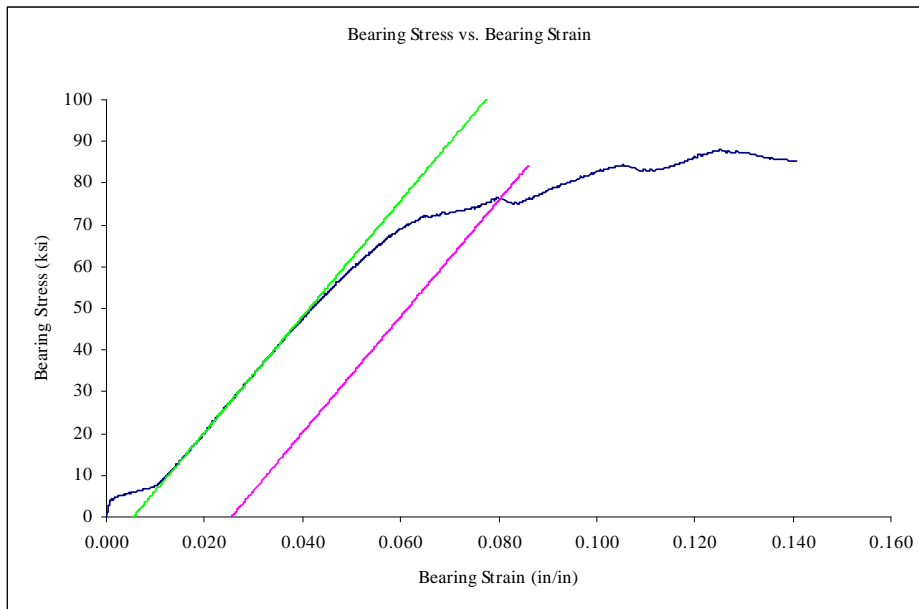


Figure 29 Bearing stress vs. bearing strain for reference position 1

Following are the load vs. deformation & bearing stress vs. bearing strain curves results for the reference position 2 as shown in figures 30 and 31.

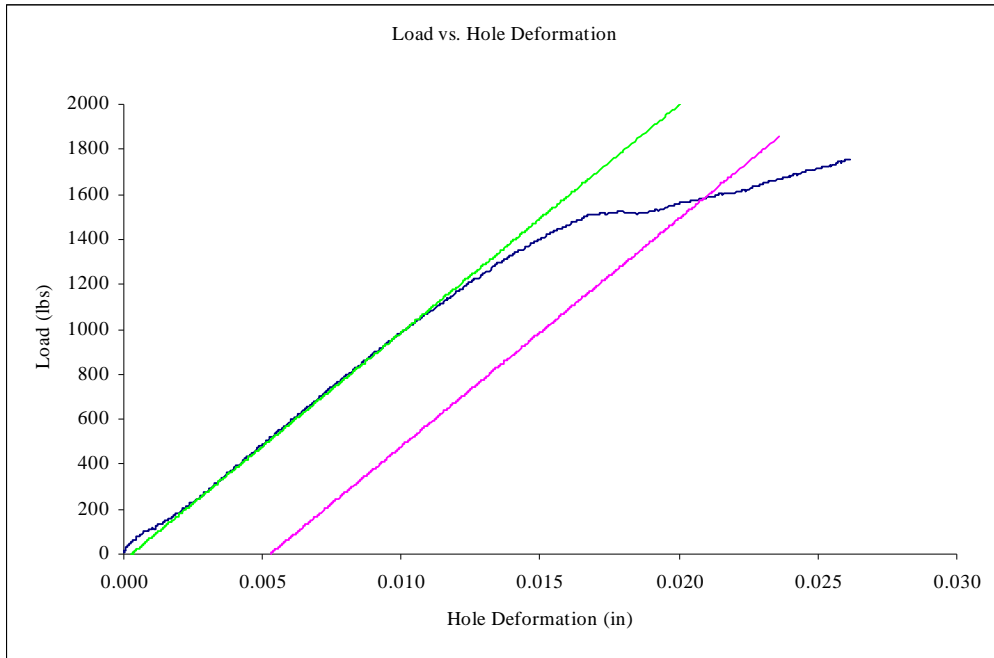


Figure 30 Load vs. deformation for reference position 2

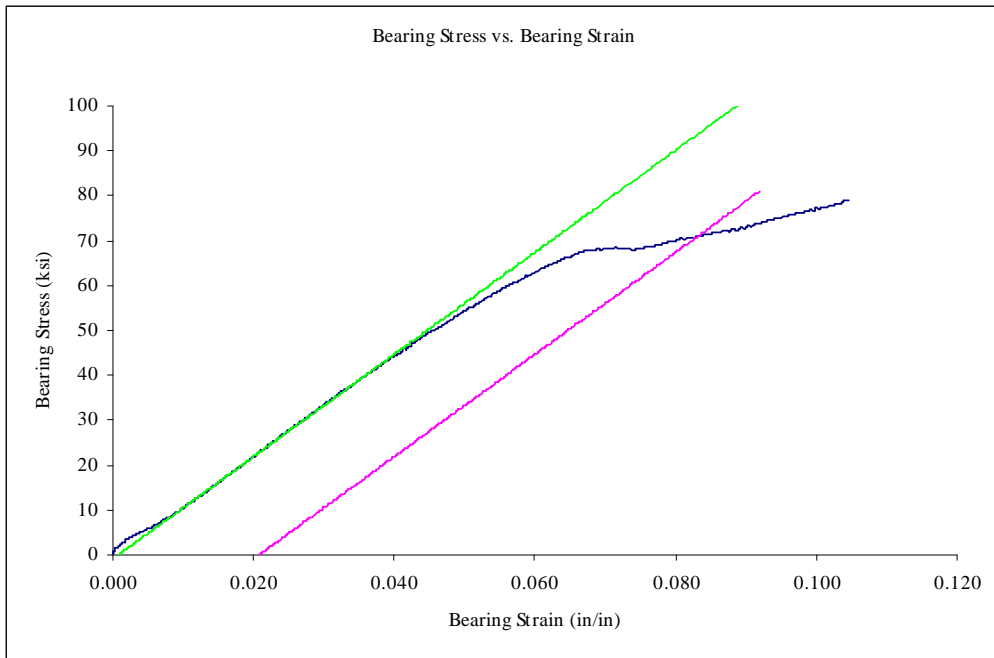


Figure 31 Bearing stress vs. bearing strain for reference position 2

Following are the load vs. deformation & bearing stress vs. bearing strain results for the reference position 2 as shown in the figures below.

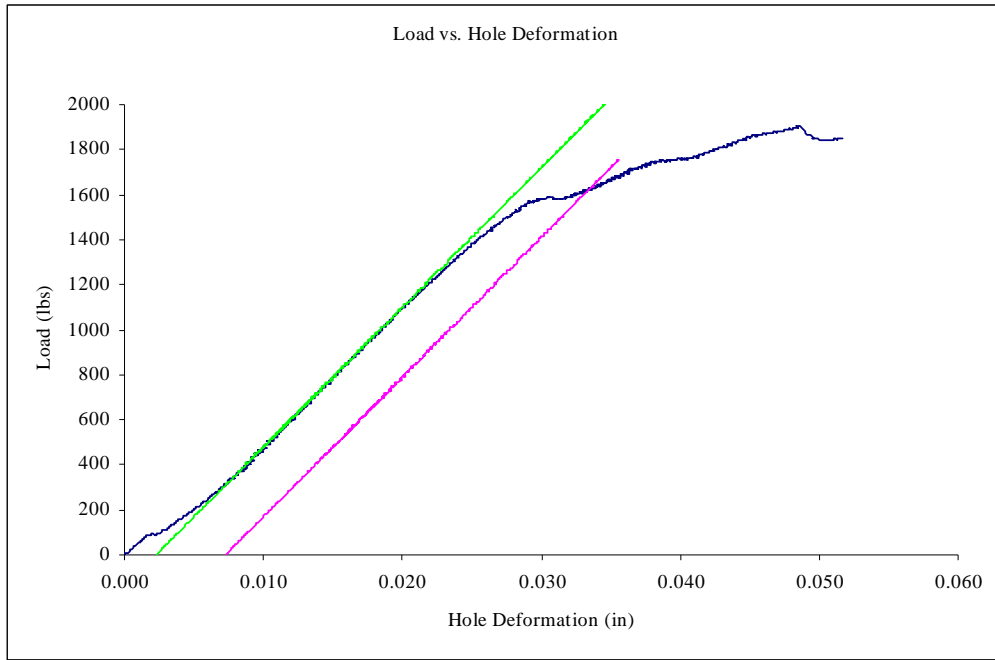


Figure 32 Load vs. deformation for reference position 3

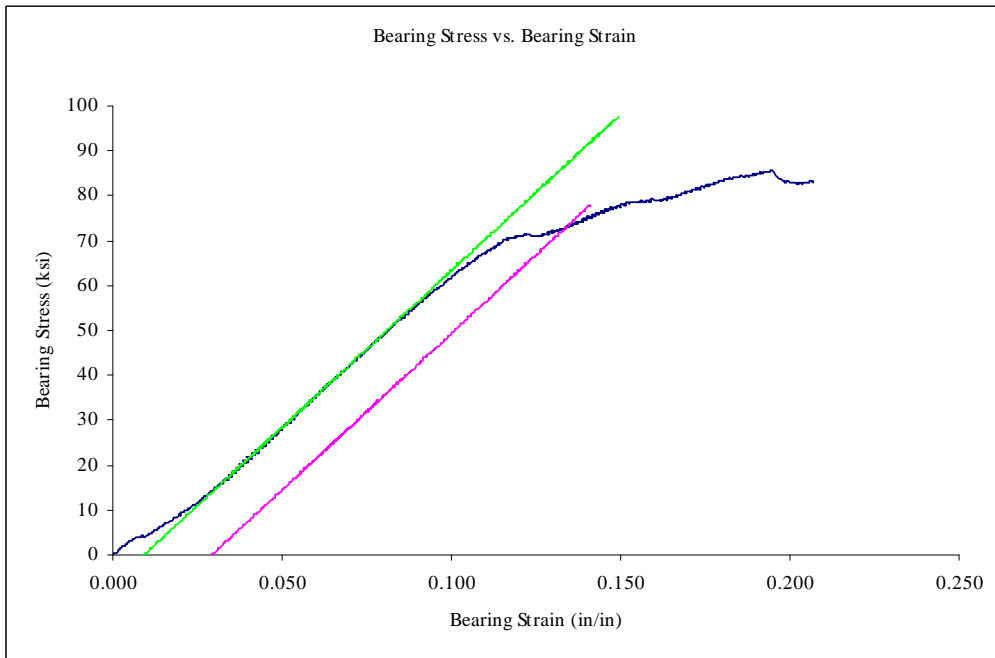


Figure 33 Bearing stress vs. bearing strain for reference position 3

Following is the bearing stress vs. bearing strain results for all the reference position 1, 2 and 3 as shown in figures 34.

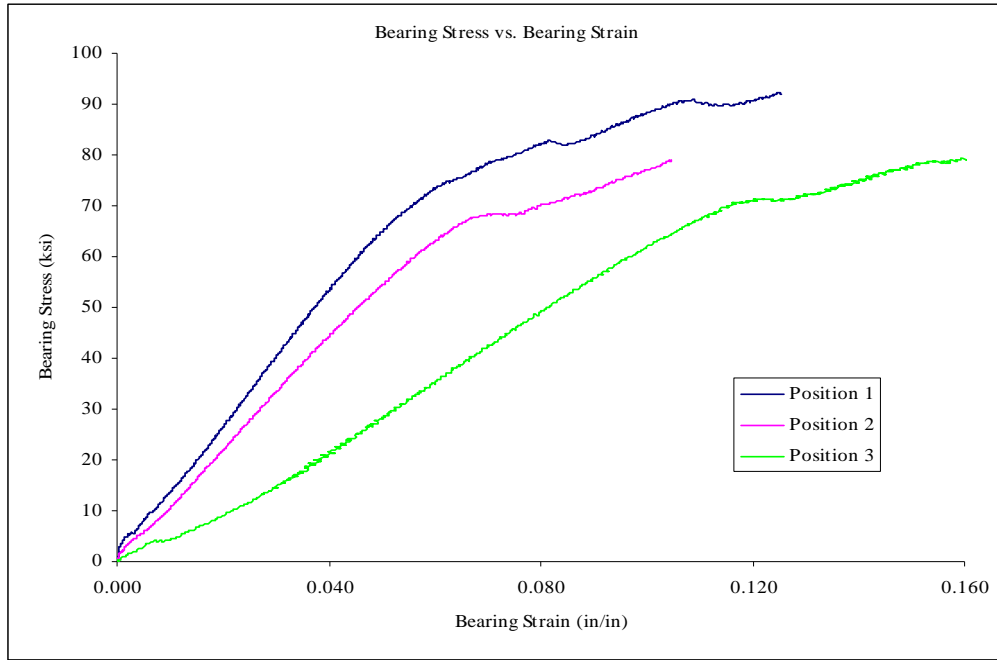


Figure 34 Bearing stress vs. bearing strain curves for all the three reference positions

A comparison of bearing stiffness and the 2% offset bearing strength of E-glass fabric material is done at various reference positions. The E-glass fabric material is compared here for the bearing stiffness and the 2 % offset bearing strength between all the three reference positions. The reference position 1 shows the maximum bearing stiffness and the reference position 3 shows the least bearing stiffness as shown in the figure 35. There is a clear trend that the bearing deformation measured in the reference position 1 i.e. right next to the center of the hole is the least and it increases as deformation is measured away from the hole i.e. the reference position 2 and 3 includes the hole deformation as well as the coupon deformation. The 2 % offset strength remains same for all the three reference positions as shown in figure 36 from which we can conclude that the bearing strength is independent of the reference position.

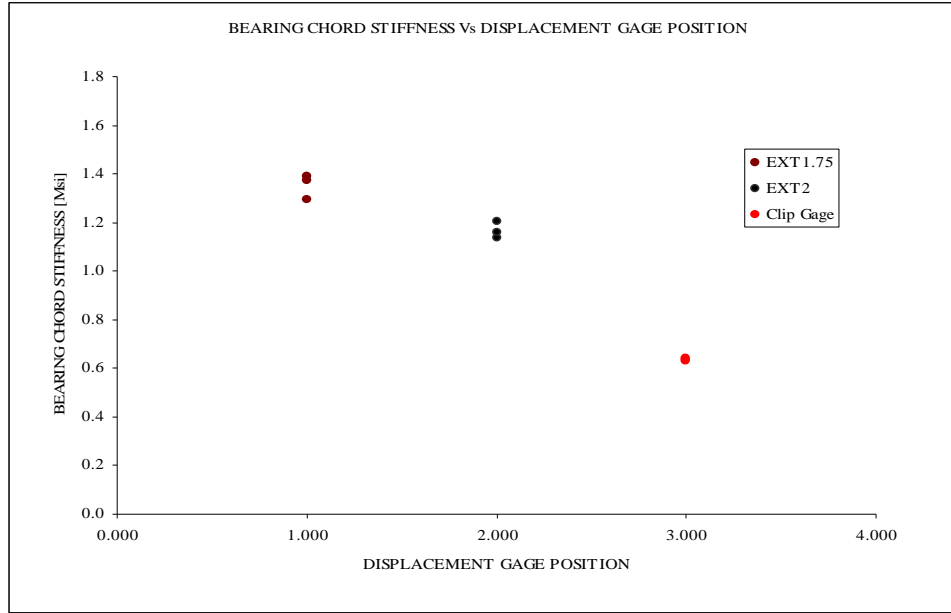


Figure 35 Bearing chord stiffness compared between three reference positions

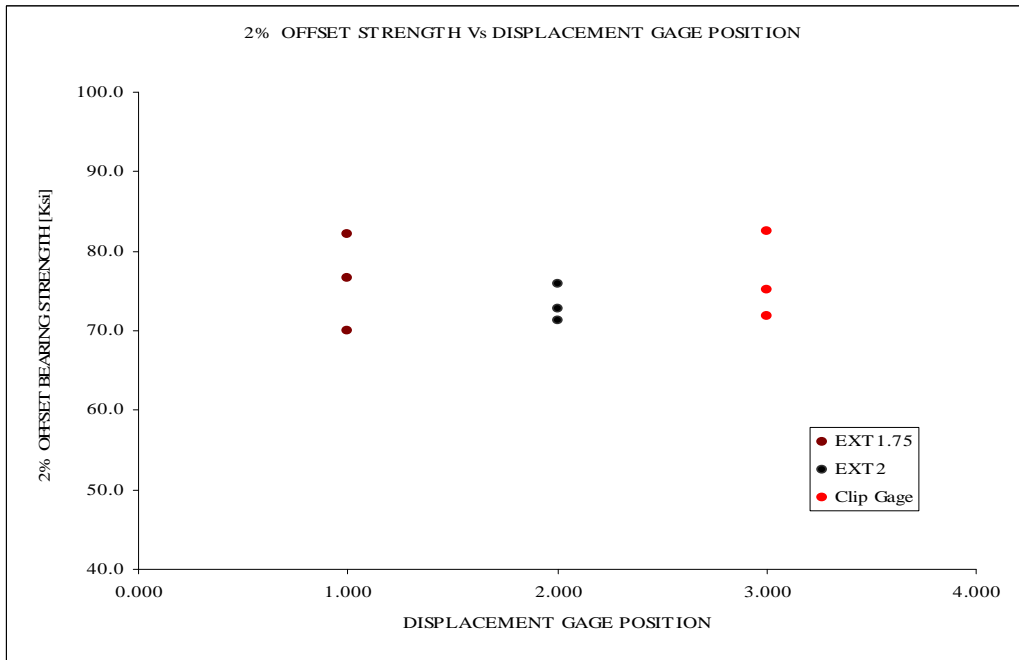


Figure 36 2% offset bearing strength compared between three reference positions

4.2 Comparison of Carbon Plain Weave Fabric and E-Glass Fabric

The two materials with Quasi-isotropic lay up sequence are compared with three different reference positions for bearing chord stiffness and 2 % offset bearing strength as shown in figure 37 and 38 respectively. It is observed that the bearing stiffness decreases from position 1 to position 3 for both the materials by 20%-30%. The carbon fiber shows 25% more stiffness than the E-glass fiber. The 2% offset values are observed to be very close for both the materials in all three reference positions. The 2 % offset strength for carbon fabric material is observed to be 20% more than the E-glass fabric as shown in figure 38. Both the materials show the similar trend that the stiffness decrease from reference position 1 to reference position 3. The 2% offset bearing strength curve is linear proving that the strength data is independent of the reference points which positive factor for the proposed method.

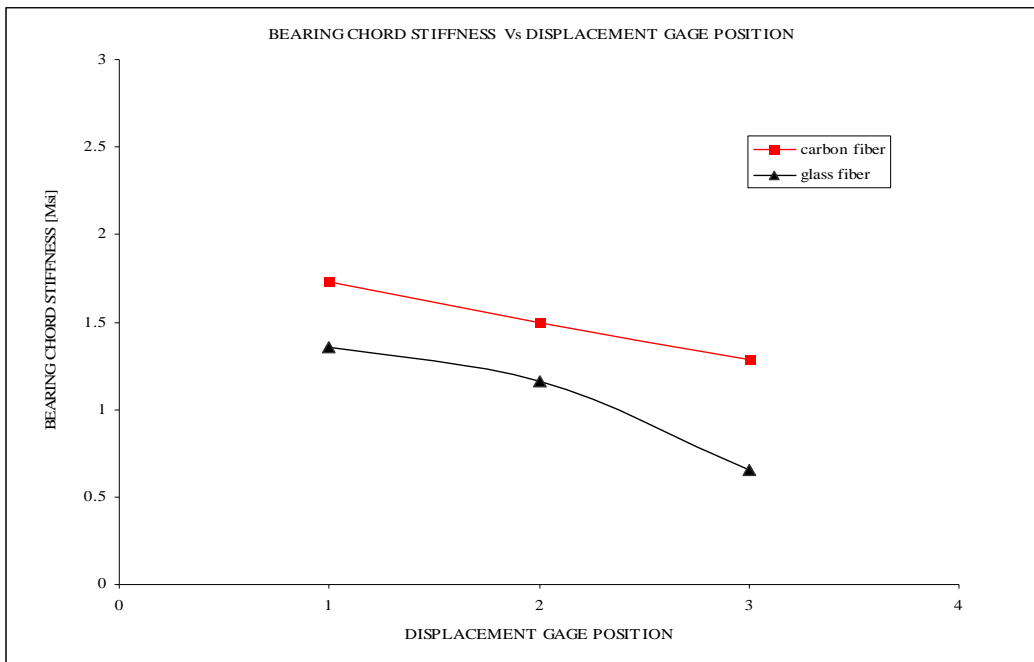


Figure 37 Bearing chord stiffness comparison between two materials and three reference positions

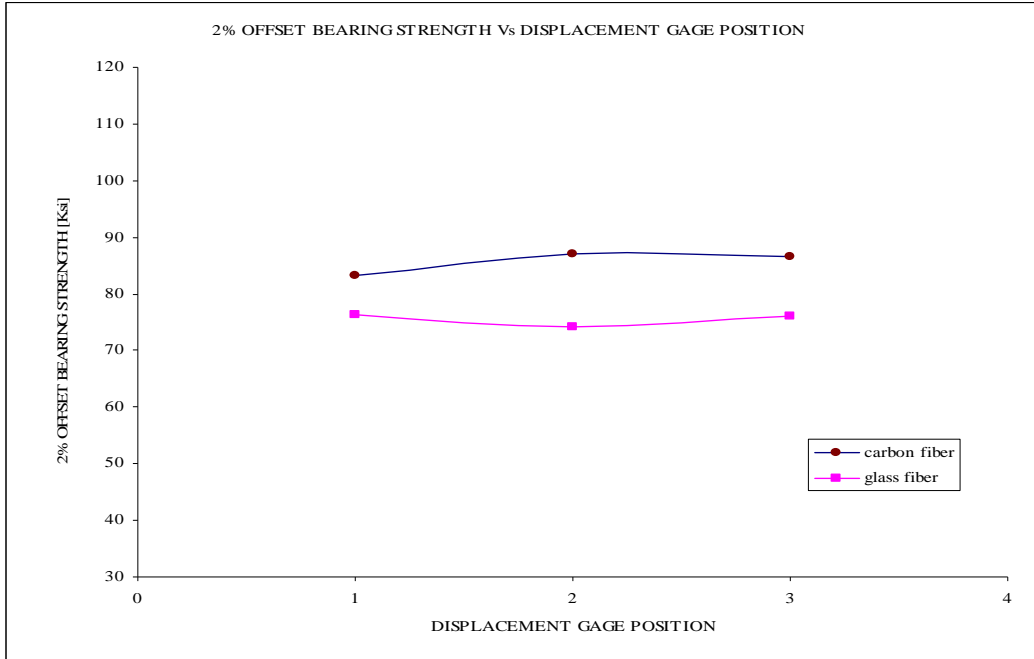


Figure 38 2 % offset bearing strength comparison between two materials and three reference positions

4.3 Rotation Factor

Out of plane rotation is a common problem with the results when we use extensometers to measure the hole deformation. The out of plane rotation can be caused by coupon misalignment, extensometer misalignment, operator error in attaching the extensometer or slippage due to rubber bands which are used to attach the extensometer to the coupon. The extensometers are attached to the sides of the coupon as shown in the figure 14(a).

The procedure which is used at present to test single shear requires a extensometer on any one side of the coupon. So this method is prone to out of plane error. The figure 39 shows the graph for load vs. actuator deformation & hole deformation. It can be observed that the hole deformation measured by extensometer 1 and extensometer 2 vary by a large margin. As we use only one extensometer, the deformation can be either one of them which proves to be a faulty result.

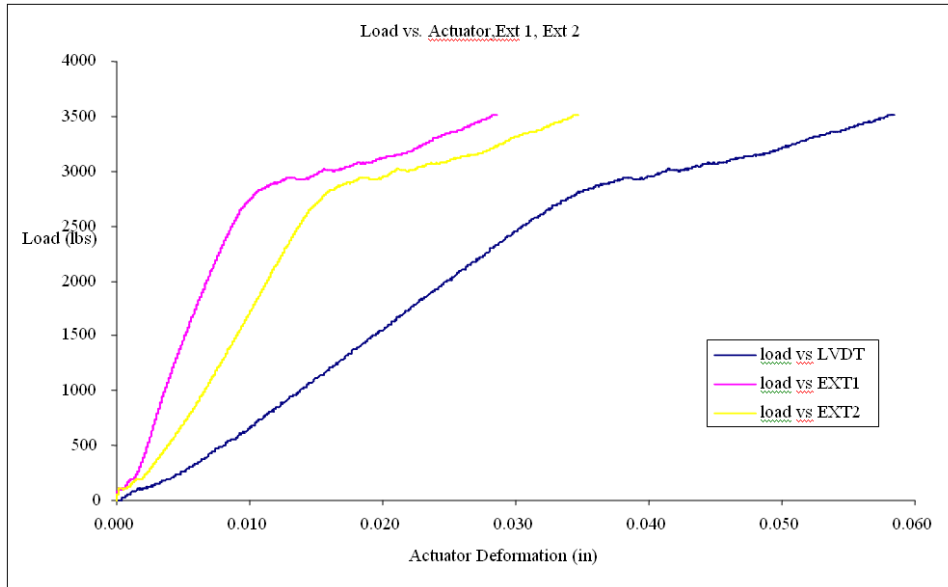


Figure 39 Load vs. actuator deformation & hole deformation for old procedure

The newly proposed ASTM D5961 procedure for testing single shear coupon requires a clip gage which is fixed using custom built attachment as shown in the figure 14(b). This procedure eliminates the out of plane rotation completely as the clip gage is fixed on the face of the specimen rather than on the edges of the specimen.

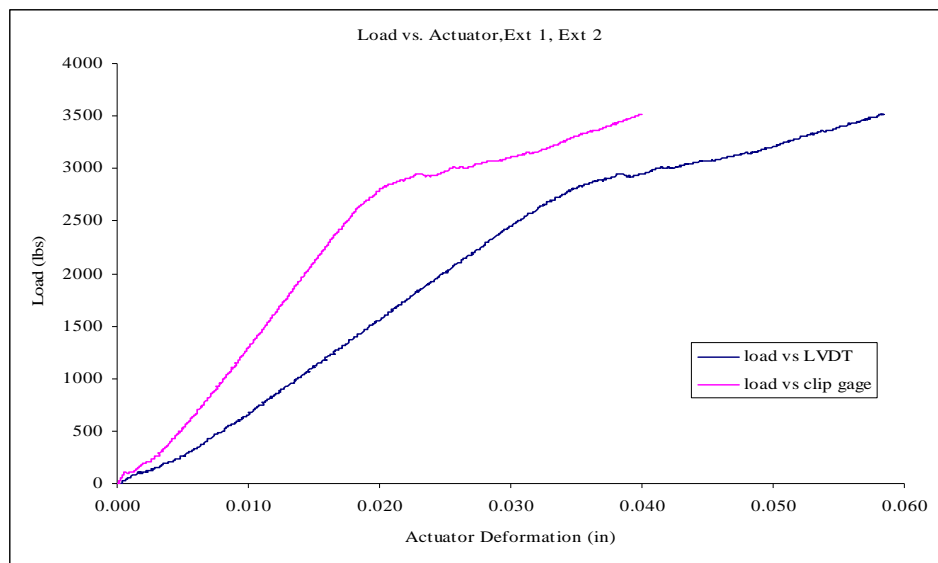


Figure 40 Load vs. actuator deformation & deformation

CHAPTER 5

COMPUTATIONAL STUDY

5.1 Introduction

The bearing test set-up is fundamentally a structure so an understanding of structure is important to study the behavior of the bearing phenomenon. The FE Model allows a parametric study of the important parameters without going for experimental study for each case. There is lot of research done in the past on the FE models by some authors[3] & [5] using various software's like ANSYS, ABAQUS and LS-Dyna.

The model studied by authors [2] show that the three-dimensional phenomena like bolt fixture etc., are of limited magnitude, so a two dimensional finite element model seemed reasonable to study the coupon deformation. It also allows parametric study of the important parameters without the excessive computational times. The FE analysis was conducted on the two dimensional model for computing the bearing single shear test with the help of LS-Dyna, a software by Livermore software technologies.

5.1 Approach

Bearing single shear test for one piece specimen is a static test. The standard test speed is 0.05 in/min. The specimen is pulled in tension for a displacement of 0.028 inches. An explicit analysis was carried out as the model was modeled for only deformation.

5.2 FE Model

The two dimensional FE model was built using MSC-PATRAN as a primary processing software. The coupon is meshed with 4 noded 2D quad elements. These shell elements with user defined integration rule is used to model 16 ply quasi-isotropic composite layup. The 2D finite element model with the detailed mesh is as shown in the figure 41.

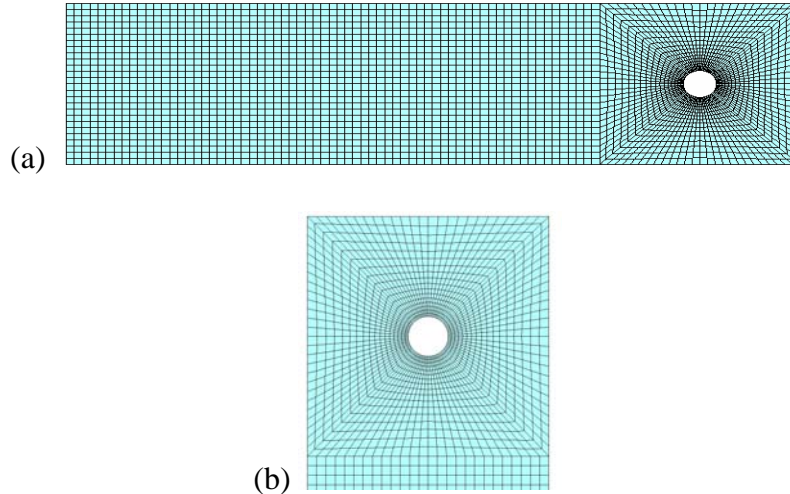


Figure 41 Two dimensional Finite element model:
 (a) Overview of the mesh; (b) Detailed mesh around hole region

5.3 Boundary Conditions and Material Properties

The appropriate material property for carbon fiber material was obtained from the NIAR agate database. The following engineering constants were used for the FE simulations: $E_x = 9.05$ Msi, $E_y = 8.63$ Msi, $\nu_{xy} = 0.048$, $G_{xy} = 0.519$ Msi. The boundary conditions applied on the coupon areas show in the figure 42. The hole region of the coupon was constrained on the top half of the hole with translational movements to simulate the rigid body conditions of the bolt shown in region (1) in figure 42. The grip region (2) of the coupon i.e. 1.5 inch at the edge of the coupon on the other side of the hole was given a displacement of 0.028 inches to simulate the tension force applied on the coupon as shown in the region (2) in figure 42.



Figure 42 Two dimensional FE model with boundary conditions

5.4 Material Model

The input file for the LS-DYNA is a file. The key file format is shown in appendix A.

- MAT_22:MAT_COMPOSITE_DAMAGE is the material model used for composite modeling without defining failure limits
- INTEGRATION_SHELL card is used with user defined integration rule to model the layup

5.5 Results and Discussion

The post processing computational procedure was run using LS-Post. The figure 41 shows the FE model. The figure 43 shows Von-Mises stress.

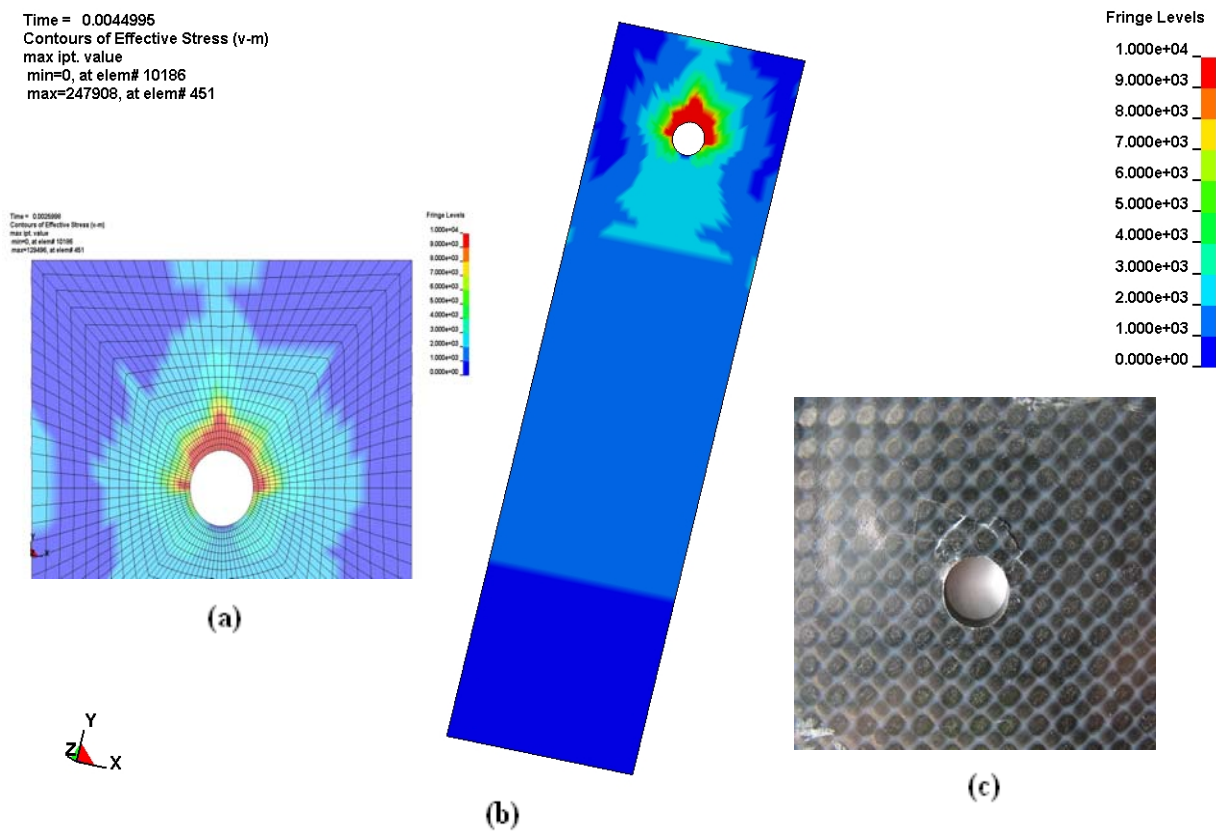


Figure 43 Distribution of Von-mises stress around the hole region: (a) Stress distribution around the hole; (b) Stress distribution in the coupon; (c) Bearing failure at the high stress region

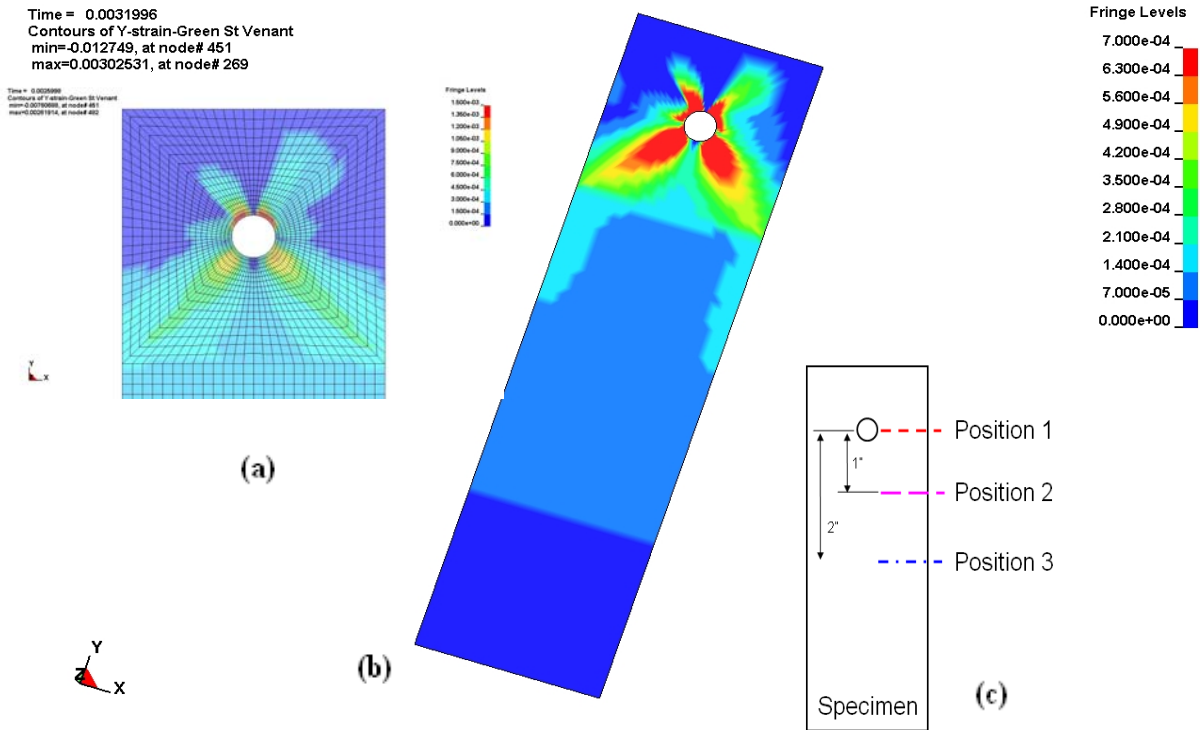


Figure 44 Y-strain distribution in the FE analyzed model: (a) Y-Strain distribution around the hole; (b) Y-Strain distribution in the coupon; (c) coupon showing three different positions

The figure 44 shows the Y-strain contour in the coupon. The strain distribution along the length of the coupon clearly shows that strain in the near vicinity of the hole towards the edge of the coupon is very minimum. The contour shows that the strain distribution becomes uniform around a distance of one inch below the hole region. The reference positions one to three are depicted in the strain contour as shown in the figure 44.

The bearing strain vs. bearing stress curves between the three positions obtained from the computational study is shown in figure 45. It should be noted that the results are valid as long as the behavior is elastic. The position 1 shows the least deformation and the position 3 shows the maximum deformation as predicted from the experimental study. The figure 46 shows the comparison for bearing chord stiffness between the experimental and the FE results. The FE results obtained in average were 20 % less than the experimental results.

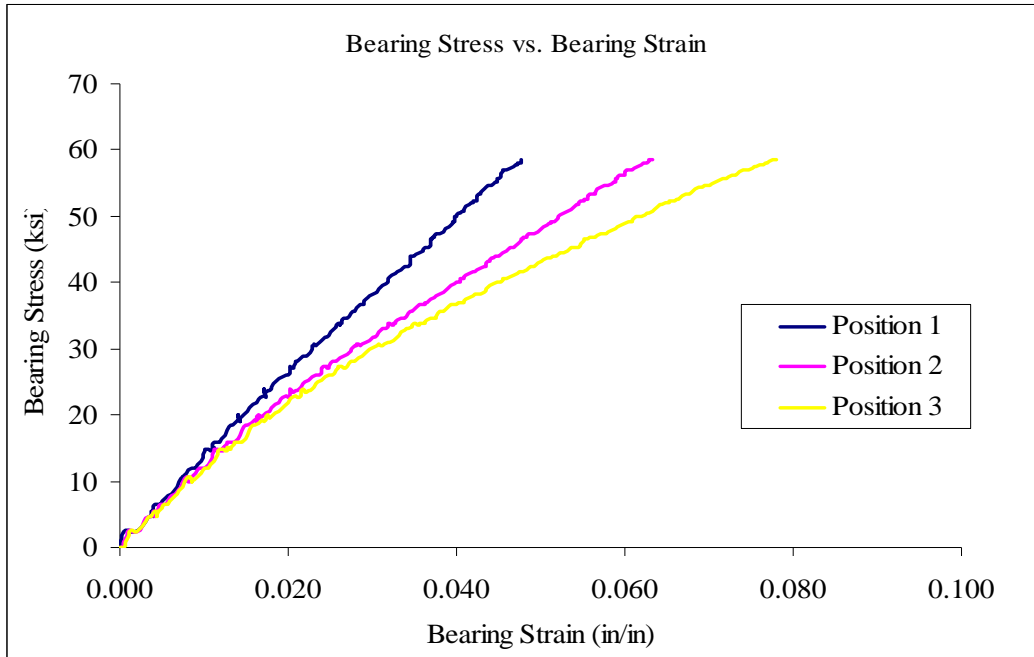


Figure 45 bearing strain vs. stress difference between the three reference positions

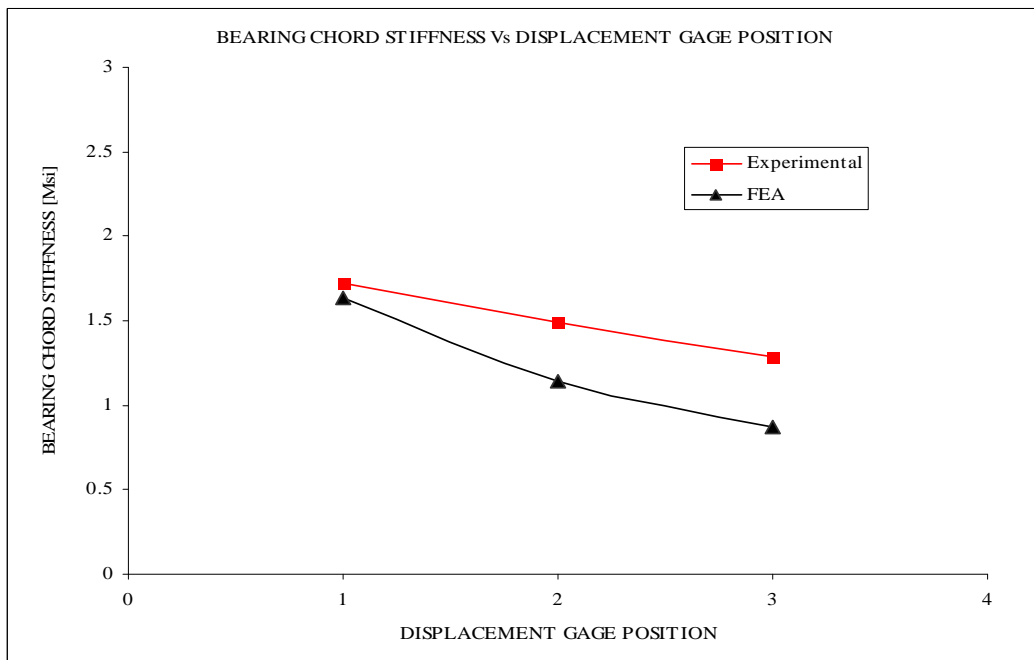


Figure 46 bearing chord stiffness compared between the experimental and FE data for all the three positions

5.6 Parametric Study

The FE model was modeled for parametric study like edge distance ratio e/d and the pitch distance ratio w/d . The edge distance ratios e/d selected for study were 2, 3 and 4. The pitch distance ratios w/d selected for study were 4, 6 and 8.

The figure 47 shows comparison between different edge distance ratios and three reference positions. Considering reference position 1 which measures only hole deformation the e/d ratio 3 gives the highest stiffness and the e/d ratio 2 gives the least. But at the reference position 3 which is much of bearing coupon deformation shows a clear trend stiffness decreases as the edge distance decreases.

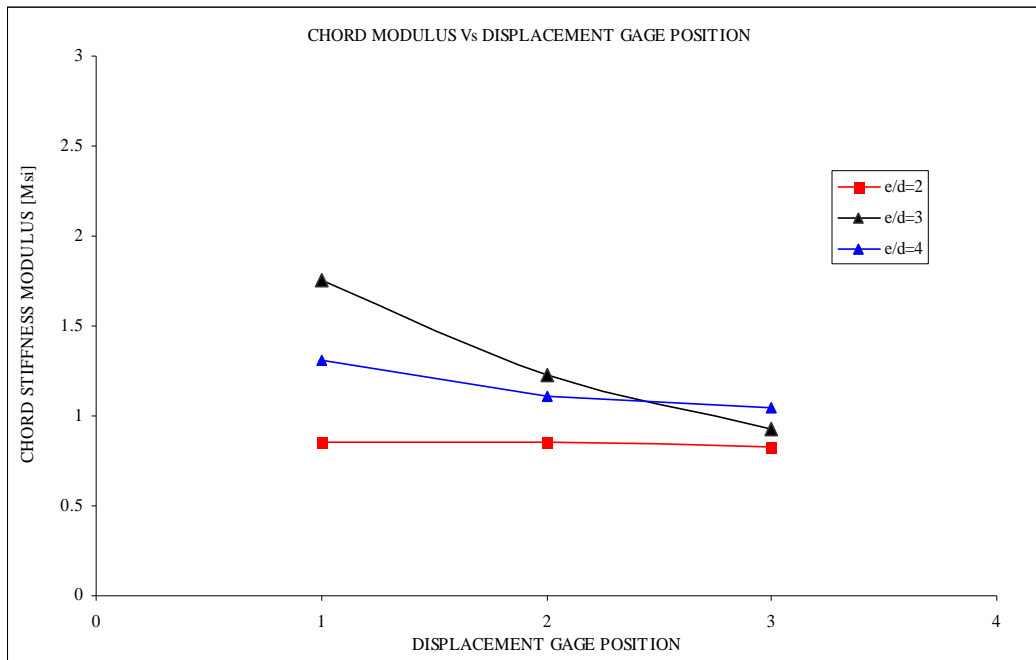


Figure 47 bearing chord stiffness vs. reference positions for end distance ratio

The figure 48 shows comparison between different pitch distance ratios and three reference positions. Considering reference position 1 which measures only hole deformation the w/d ratio 6 gives the highest stiffness and the w/d ratio 8 gives the least. But at the reference position 3 which is much of bearing coupon deformation shows a clear trend stiffness decreases as the width of the coupon increases.

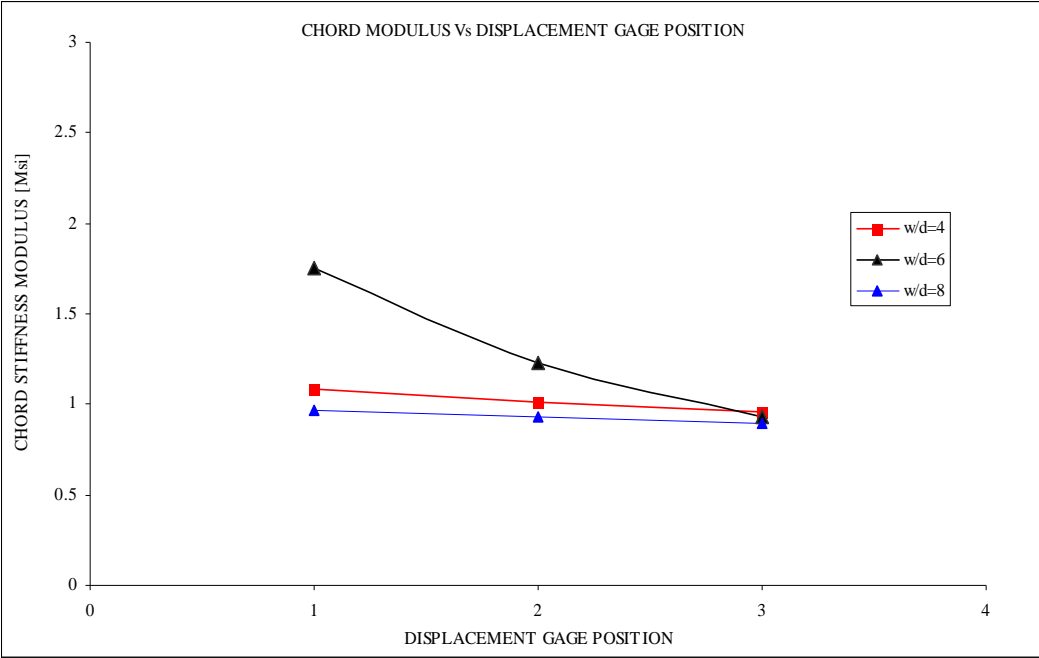


Figure 48 bearing chord stiffness vs. reference positions for pitch distance ratio

CHAPTER 6

STATISTICAL ANALYSIS OF COMPUTATIONAL DATA

To validate FE analysis results it is necessary to conduct statistical analysis to draw meaningful conclusions. Statistical analysis helps to remove errors from the obtained results, also providing validity to the FE results. This gives the confidence that FE methods, results and conclusion are sound and valid.

The statistical analysis was conducted using Stat-Ease. The factors considered were reference positions and parametric ratios. The statistical design selected for this study was general factorial since the study had two factors. These factors consisted of three reference positions, position 1, 2 & 3, and six ratios $e / d = 2, 3 \text{ \& } 4$, $w / d = 4, 6 \text{ \& } 8$ as factor 1 and factor 2 respectively. The statistical results are discussed in the following sections.

6.1 Statistical Design Matrix

Based on the general factorial design the Stat-Ease software generated an experimental matrix where the experimental data for analysis was entered. Table 5.1 shows the statistical design matrix.

TABLE 3
STATISTICAL DESIGN MATRIX

STD	RUN	FACTOR 1 A:POSITIONS	FACTOR 2 B:RATIO	RESPONSE 1 BEARING CHORD STIFFNESS (Msi)
1	10	position 1	e/d=2	0.852
2	1	position 2	e/d=2	0.850
3	3	position 3	e/d=2	0.824
4	18	position 1	e/d=3	1.751
5	8	position 2	e/d=3	1.227
6	17	position 3	e/d=3	0.928
7	2	position 1	e/d=4	1.313
8	14	position 2	e/d=4	1.106
9	16	position 3	e/d=4	1.042
10	11	position 1	w/d=4	1.081
11	5	position 2	w/d=4	1.008
12	15	position 3	w/d=4	0.954
13	6	position 1	w/d=6	1.751
14	12	position 2	w/d=6	1.227
15	9	position 3	w/d=6	0.928
16	4	position 1	w/d=8	0.964
17	13	position 2	w/d=8	0.932
18	7	position 3	w/d=8	0.896

6.2 Statistical Output Analysis

Once the data has been entered to the statistical design matrix, significance of the factors on the responses is analyzed using ANOVA, which is statistical output. To identify the effect of

factors on the response, ANOVA analysis is conducted at a specific significance level or confidence interval α of 0.05. The main outputs of this statistical analysis are ANOVA table and the diagnostic plots. This analysis consisted of only one response the bearing chord stiffness.

6.2.1 ANOVA Output for bearing chord stiffness

TABLE 4

ANOVA TABLE FOR BEARING CHORD STIFFNESS

SOURCE	SUM OF SQUARES	DEGREES OF FREEDOM	MEAN SQUARE	F VALUE	PROB > F	
Model	0.951	7	0.136	3.838	0.0274	significant
A	0.391	2	0.196	5.529	0.0242	
B	0.560	5	0.112	3.161	0.0572	
Residual	0.354	10	0.035			
Cor Total	1.305	17				

From the ANOVA table for the average delamination depth it is seen that the model selected is significant since the prob>F value 0.0274 is less than the significance level value 0.05, which indicates that the factors considered in the model are significant. Here the model terms (factors) A and B refer to the reference positions and the parameter ratios respectively. The ANOVA table shows that the response bearing chord stiffness mainly depends on the individual effect of the factors and not on the interaction effect of the factors. The ANOVA confirms the decrease in bearing chord stiffness from reference position 1 to position 3 as seen in the graphs plotted.

6.2.2 Residual analysis for delamination depth

In order to check the validity of the ANOVA model, the residuals plots were examined. The residual plots include normal probability plot, outlier plot, residuals vs. factors and residuals vs. predicted.

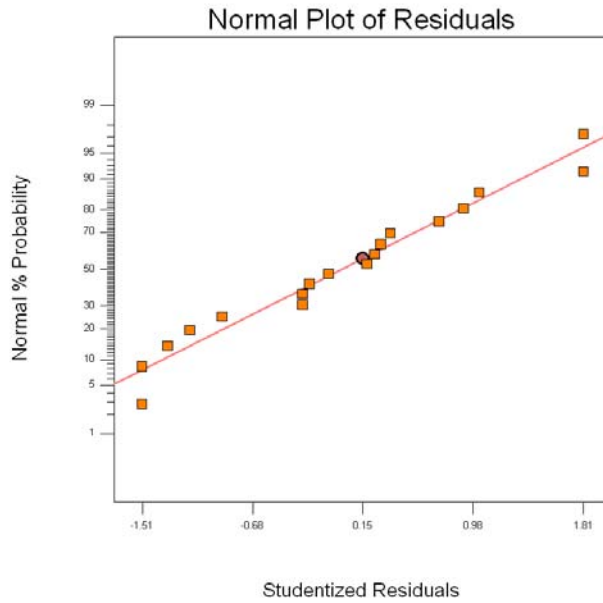


Figure 49 Normal probability plot: Bearing chord stiffness

The normal plot as shown in figure 49 shows that there is no serious violation of the ANOVA assumptions regarding the distribution of the experimental errors.

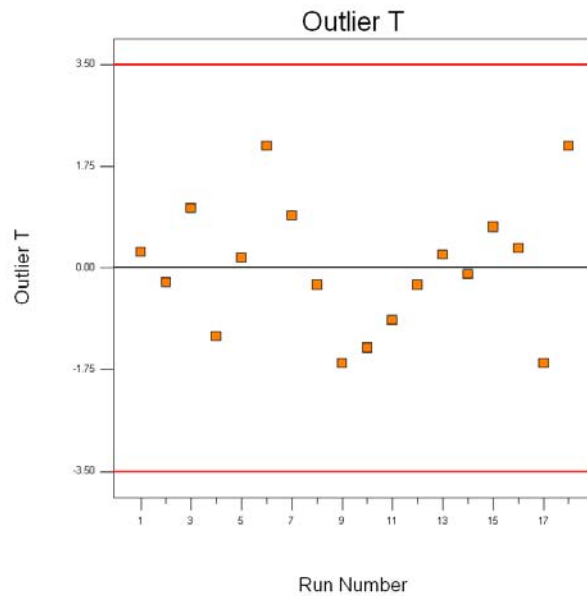


Figure 50 Outliner plot: Bearing chord stiffness

The outlier plot as shown in Figure 50 shows that there are no outliers in observed in the experiment.

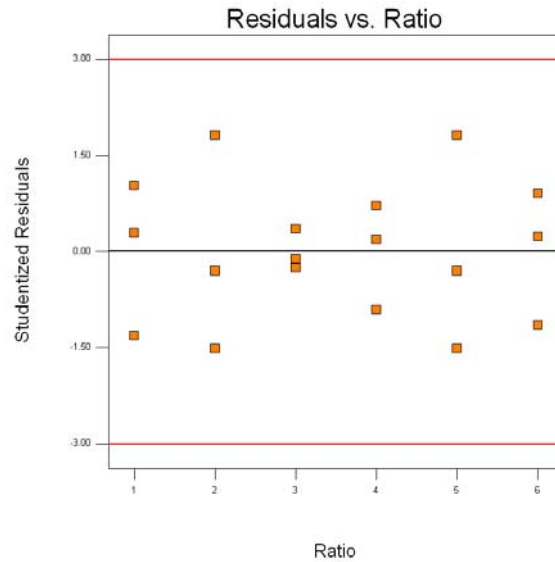


Figure 51 Residuals vs. Parameter ratio: Bearing chord stiffness

As per Residuals Vs Ratio plot as shown in figure 51 it is observed that the residuals are scattered without any specific pattern and no funnel shape is found. Hence, there are no violations of constant variance and independency assumptions of the ANOVA procedures.

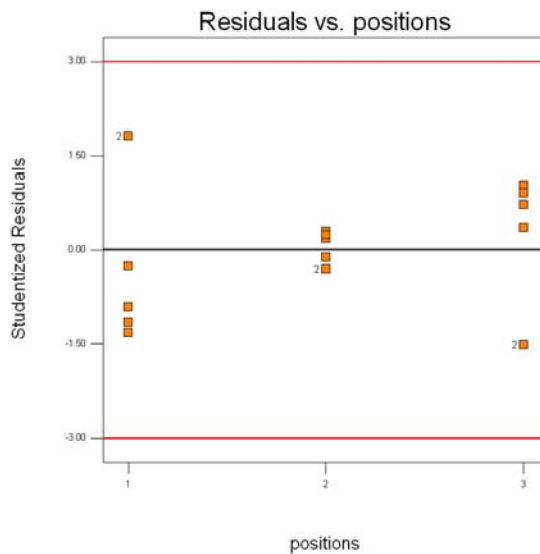


Figure 52 Residual vs. reference positions: Bearing chord stiffness

The Residual plots shown from Figure 52 show that the residual values do not follow any trend or funnel shape and hence there is no violation of the constant variance assumption of ANOVA.

6.2.3 Factor effects of bearing chord stiffness

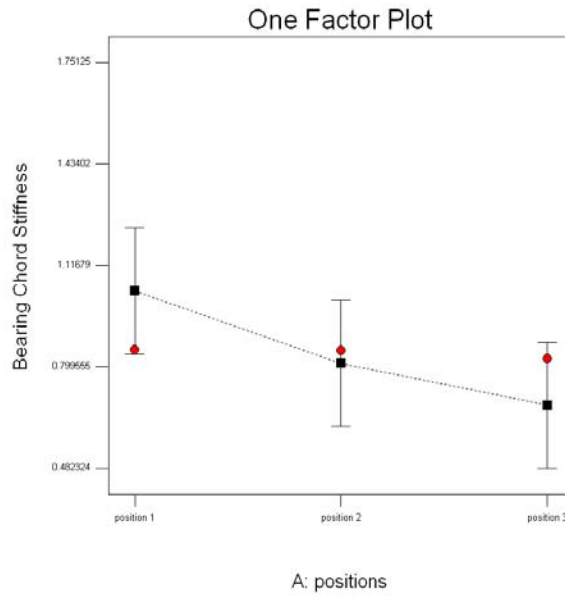


Figure 53 Effect of reference positions on bearing chord stiffness for $e/d = 2$

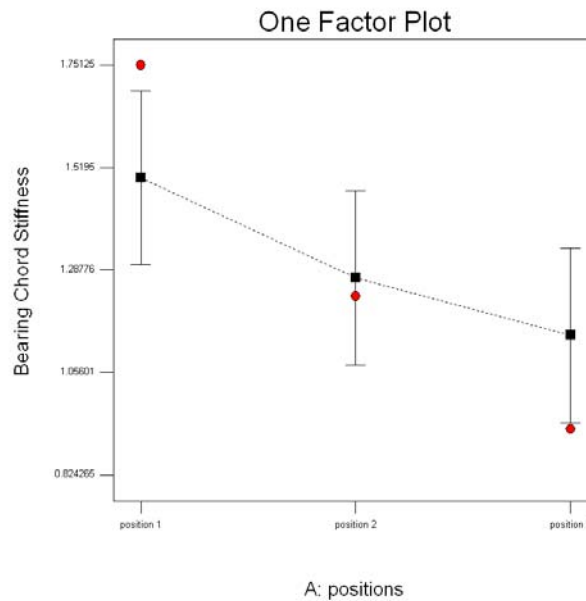


Figure 54 Effect of reference positions on bearing chord stiffness for $e/d = 3$

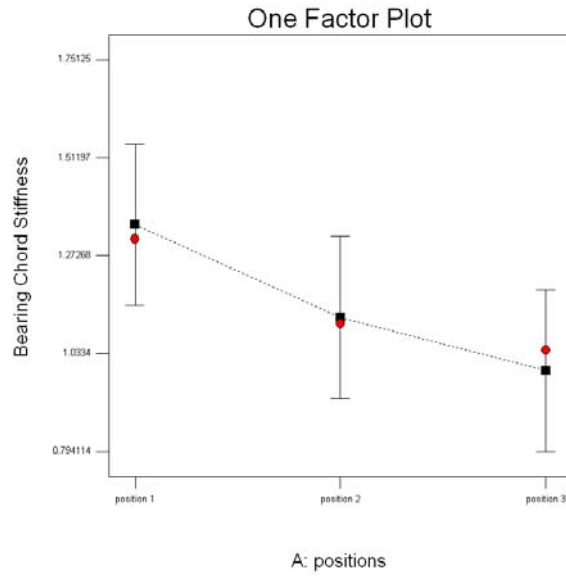


Figure 55 Effect of reference positions on bearing chord stiffness for $e/d = 4$

These factor effects show that the bearing stiffness decreases as the edge to diameter ratio decreases, and the same decreases from reference position 1 to reference position 3. This trend has been previously shown in the experimental results.

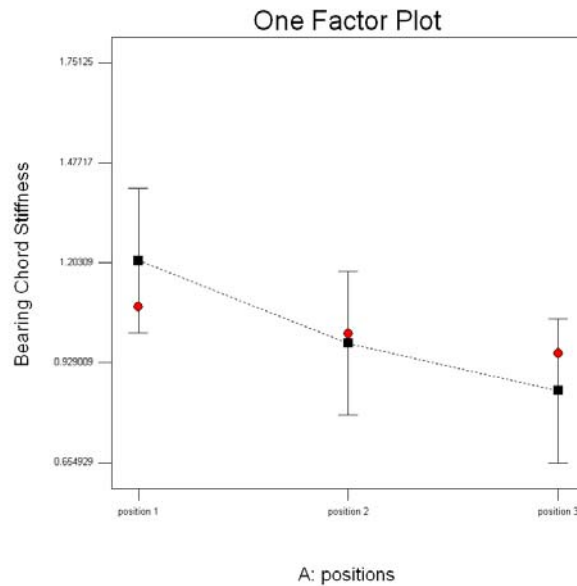


Figure 56 Effect of reference positions on bearing chord stiffness for $w/d = 4$

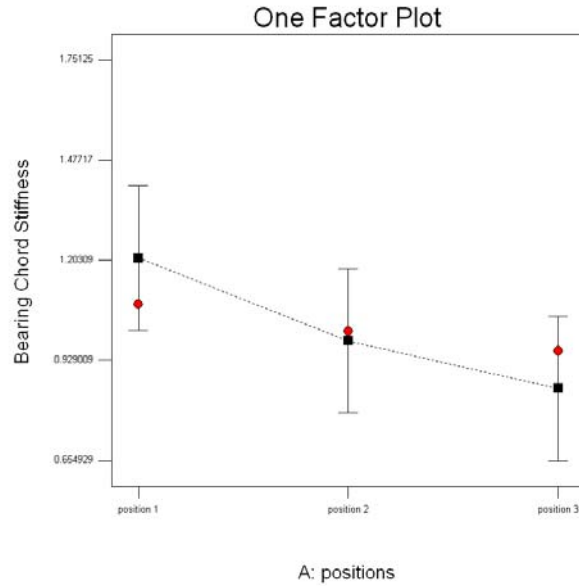


Figure 57 Effect of reference positions on bearing chord stiffness for $w/d = 6$

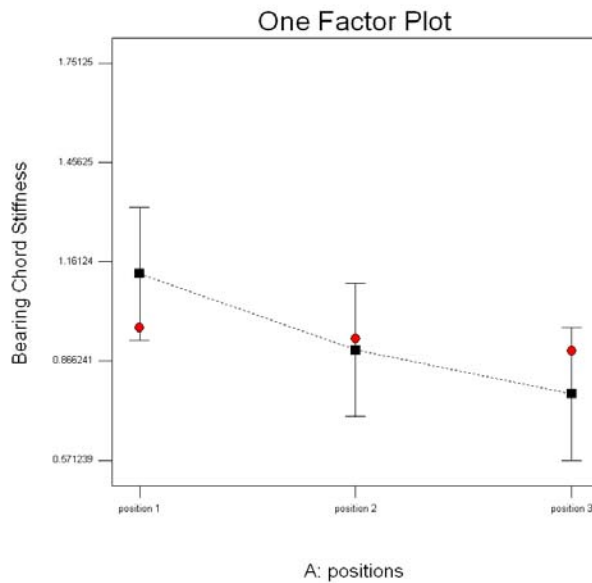


Figure 58 Effect of reference positions on bearing chord stiffness for $w/d = 8$

These factor effects show that the bearing stiffness decreases as the width to diameter ratio decreases, and the same decreases from reference position 1 to reference position 3. This trend has been previously shown in the experimental results.

CHAPTER 7

CONCLUSIONS AND RECOMMENDATIONS

7.1 Conclusions

This study dealt with optimizing the displacement gage position in the ASTM D5961: procedure 'C'. Experiments were carried out considering two test procedures, three reference positions and two material types. A FE model was validated to perform a set of parametric studies. This parametric study data was used to find out factors affecting the results using statistical analysis.

The single shear test on single piece specimen i.e. ASTM D5961 Procedure 'C' tests were conducted successfully for two materials and in all the three reference positions. The deformation measured at position 3 is nearly 20-30% more than the deformation measured at position 1 which shows that the position 2 and position 3 includes the hole deformation as well as the coupon deformation. The stiffness and the strength values for the glass fiber is 20% lesser than the carbon fiber as predicted because the number of plies in glass fiber is half the plies in the carbon fiber material and the carbon fibers are more stiffer than the glass fibers. The chord stiffness decreases in the similar trend for both the materials from reference position 1 to reference position 3. The 2% offset bearing strength shows a linear trend for both the materials between the three reference positions. All the tested coupons resulted in bearing failure which validates the experiment for its correctness. The out of plane rotation is completely eliminated in the ASTM D5961 proposed procedure leading to more accurate bearing deformation results.

The FE model was a source for future research which was done to study various parameters like edge distance ratio and pitch distance ratio. A FE 2D model was developed to validate the quasi isotropic carbon fiber material simulated to get the deformation in all the three

reference positions. The finite element analysis show a variation of 25% for the bearing chord stiffness values in comparison with the experimental results. The effect of edge distance ratio and pitch distance ratio parameters were studied successfully. The edge distance ratio of 3 showed the maximum stiffness i.e. least deformation and the edge distance ratio of 2 showed the least stiffness i.e. maximum deformation at reference positions 1 and 2. The bearing chord stiffness decreases from reference position 1 to reference position 3 for edge distance ratio 3, similarly the other two ratios 2 and 4 show the same trend but not significantly as the ratio 3. The pitch distance ratio 6 showed the maximum stiffness i.e. least deformation and the pitch distance ratio 8 showed the least stiffness i.e. maximum deformation.

The FE parametric study showed that the bearing stiffness significantly differ for only edge distance ratio 3 and pitch distance ratio 6 between the three reference positions which is the standard configuration of the testing coupon.

The statistical analysis was carried out to find out significant factors for the bearing stiffness data obtained from computational study. It was evident that the bearing stiffness significantly varies from reference position 1 to reference position 3 and for only edge distance ratio of 3 and pitch distance ratio of 6 as seen in the computational study.

The single shear testing method for single piece specimen proposed by ASTM D5961 is recommended for the future research. The 2% offset bearing strength which is of more importance for the engineers than the bearing chord stiffness is found to be equal for both the procedures whereas the stiffness readings in this procedure are more conservative.

The proposed procedure is easy to conduct by the operator. The out of plane rotation was completely eliminated in this when compared to the old procedure. Thus proposed method is recommended for the future research and testing.

7.2 Recommendations

The experiments were carried out in ambient room temperatures. Similar experiments can be conducted in elevated temperatures from -65°F to 350°F to study the response of the bearing hole in different temperatures to simulate real time applications of the composite joints. The experiments were confined to single hole diameter as it is a standard configuration for testing procedure 'C'. More detailed FE study is recommended considering factors like torque and different hole tolerances. More detailed factors can be considered to calculate the stresses calculated in the FE-model, and apply several failure criteria to predict other modes of failure.

REFERENCES

REFERENCES

- [1] Anonymous, Designation: D5961/D5961M-05, "Standard Test Method for Bearing Response of Polymer Matrix composite Laminates," ASTM Standards, 2006.
- [2] B. Vangrimde and R. Boukhili, "Analysis of the bearing test for the polymer matrix composites: bearing stiffness measurement and simulation," *Composite structures*, Vol. 56, pp. 359-374, 2002.
- [3] Matthews, F.L., and Camanho, P.P., "A Progressive Damage Model for Mechanically Fastened Joints in Composites Laminates," *Journal of Composite Materials*, 2000.
- [4] Chang, F.K., and Sun, H.T., "The Response of Composite joints with bolt Clamping Loads," *journal of Composite Materials*, Vol. 36, No.1, 2002.
- [5] Jones, R.M., Taylor and Francis, "*Mechanics of Composite Materials*," Philadelphia, 1999.
- [6] Naik, V.A., and Crews, J.H., "Failure Analysis of a Graphite /Epoxy Laminate subjected to Bolt Bearing Loads," NASA Technical Memorandum 86297, August 1984.
- [7] Pascoe, J., and Smith, P., "The Effect of stacking Sequence on the bearing strengths of Quasi-Isotropic Composite Laminates," *Composite Structures*, Vol. 6, pp. 1-20, 1996.
- [8] Naik, V.A., and Crews, J.H., "Failure Analysis of a Graphite /Epoxy Laminate subjected to Bolt Bearing Loads," NASA Technical Memorandum 86297, August 1984.
- [9] Takaka, T., "Mechanical Behavior of Bolted Joint in Various Clamping Configurations", *Journal of pressure vessel technology*, Vol. 120, 1998, pp226-231.
- [10] Schyprykevich, P., "Characterization of Bolted Joint Behavior: Accomplishment at Standardization," *Journal of Composite Technology and Research*. MIL-HDBK-17, Vol.17, July 1995, pp. 260-270.
- [11] Jurf, R.A., and Vinson, J., "Failure Analysis of Bolted Joints in Composite Laminates," *Composite Materials Testing and Design*, ASTM, Philadelphia, Vol.9, pp. 165-190, 1990.
- [12] VanTooren, D., Gleich, D.M., and Buekers, A., Characteristics and Testing, "Structural bonded joint analysis: An overview," *Adhesive Joints: Formation*, Vol. 2, 2001, pp. 159-199.
- [13] Adams, R. D., and Wake, W.C., *Structural Adhesive Joints in Engineering*, Chapman & Hall, 1997, pp.119-166.